hypermethylation at the *Sall3* locus occurs in the placenta of mice cloned with other types of cells (Fig. 1C). In the placenta of a female-fibroblast clone (#18, B6D2F1), the locus was hypermethylated compared with NM controls (72% vs. 54%). Similarly, in (B6xJF1)F1 mice, the placentas of a male-fibloblast clone (#19) and a female-fibroblast clone (#20) showed hypermethylation compared with controls (65%, 58% vs. 45% and 43%, respectively). Thus, the *Sall3* locus is hypermethylated regardless of the genetic background, sex and type of the nuclear donor cells.

Oocyte manipulation and *in vitro* culture do not affect the methylation status of the Sall3 locus

To control for the possibility that the *in vitro* culture of oocytes and embryos by themselves may trigger abnormal DNA methylation at gene loci (Doherty *et al.* 2000), we examined the methylation status of the placentas of fetuses produced by ICSI and IVF. We found that the degrees of methylation of the *Sall3* locus in placentas of ICSI and IVF fetuses were 53 ± 4% and 52 ± 6%, respectively (Fig. 1D). Thus, the placentas of mice produced after *in vitro* manipulation were not significantly different from those of NM controls as far as the methylation status of the *Sall3* locus is concerned.

The extent of DNA methylation was confirmed by quantitative genomic PCR (Fig. 1E). The placental genome of the NM, IVF and ICSI controls showed 56, 54, and 58% methylation, respectively, at the *Not*I site of the *Sall3* locus. Similarly, clone #4, which showed moderate hypermethylation by Southern blotting was 59% methylated. In contrast, clones #3 and #6 showed hypermethylation (69%) compared with the NM, IVF and ICSI controls.

DNA methylation level of the Sall3 locus correlates with placental weight in cloned mice

To evaluate the relationship between methylation aberration and placental phenotype, methylation rate and placental weight of each cloned placenta are plotted in Fig. 1(F). There was a positive correlation between the extent of hypermethylation of the *Sall3* locus and placental weight in cloned mice ($r = 0.61$, $P < 0.1$).

Methylation status of CpGs within the Sall3 T-DMR

We analysed the methylation status of the *Sall3* locus in ES and TS cells by bisulfite sequencing to determine the size of the *Sall3* T-DMR. The T-DMR was 904 bp in length and located in a region just 5′ of the *Not*I site extending to 3′ region that is highly homologous with human (Fig. 2A). The T-DMR containing 31 CpGs was hypermethylated in TS cells compared with ES cells, as previously reported (Shiota *et al.* 2002). Bisulfite sequencing analysis of the *Sall3* T-DMR revealed hypermethylation in the placenta of cloned mouse (#15) throughout the T-DMR (Fig. 2B). Comparison between the human and mouse *SALL3/Sall3* locus showed the sequence homology in T-DMR as well as promoter and exon 1 (Fig. 2C). Although the methylation status of the *Not*I site was about 50% in the control placentas (Fig. 1B), the methylation pattern of the whole T-DMR was unlike the pattern of typical imprinted genes. In imprinted genes, differentially methylated regions would show about 50% methylation within whole regions.

Methylation status of the Sall3 locus in the brain and liver of cloned fetuses at term

The *Sall3* gene was suggested to play important physiological roles in various tissues (Ott *et al.* 1996). To address the question whether the epigenetic error at the *Sall3* locus of cloned mice may occur in other tissues, we investigated the methylation status of the *Sall3* locus in the brain and liver of cloned fetuses at term by Southern blotting (Fig. 3). The *Sall3* locus was not methylated in the brain and liver in the control as reported previously (Shiota *et al.* 2002). The *Sall3* T-DMR was hypomethylated in these tissues of the clones as in the control, although the liver of clones was slightly methylated. This shows that the *Sall3* locus is methylated specifically in the placenta, perhaps in the trophoblast cell lineage, as previously reported (Ohgane *et al.* 2001; Shiota *et al.* 2002) and that the aberrant hypermethylation occurs uniquely in the placenta of cloned mice.

Discussion

Sall3 mRNA was barely expressed in TS cells and did not show dramatic change after differentiation (data not shown). The mouse *Sall3* T-DMR covers the region highly homologous to human genomic sequence in equivalent location (Fig. 2B,C), suggesting that this region has important functions in both species. Human chromosome 18q is one of the regions which are lost frequently in cancer cells, and its loss is often related to abnormal genome-wide hypomethylation (Schulz *et al.* 2002). The human 18q23 region containing the *SALL3* locus is likely to be responsible for the 18q deletion syndrome (OMIM #605079 and 601808) (Kohlhase *et al.* 1999). This region includes the *MBP*, *GALR1* and *NFATC* genes which could be responsible for several

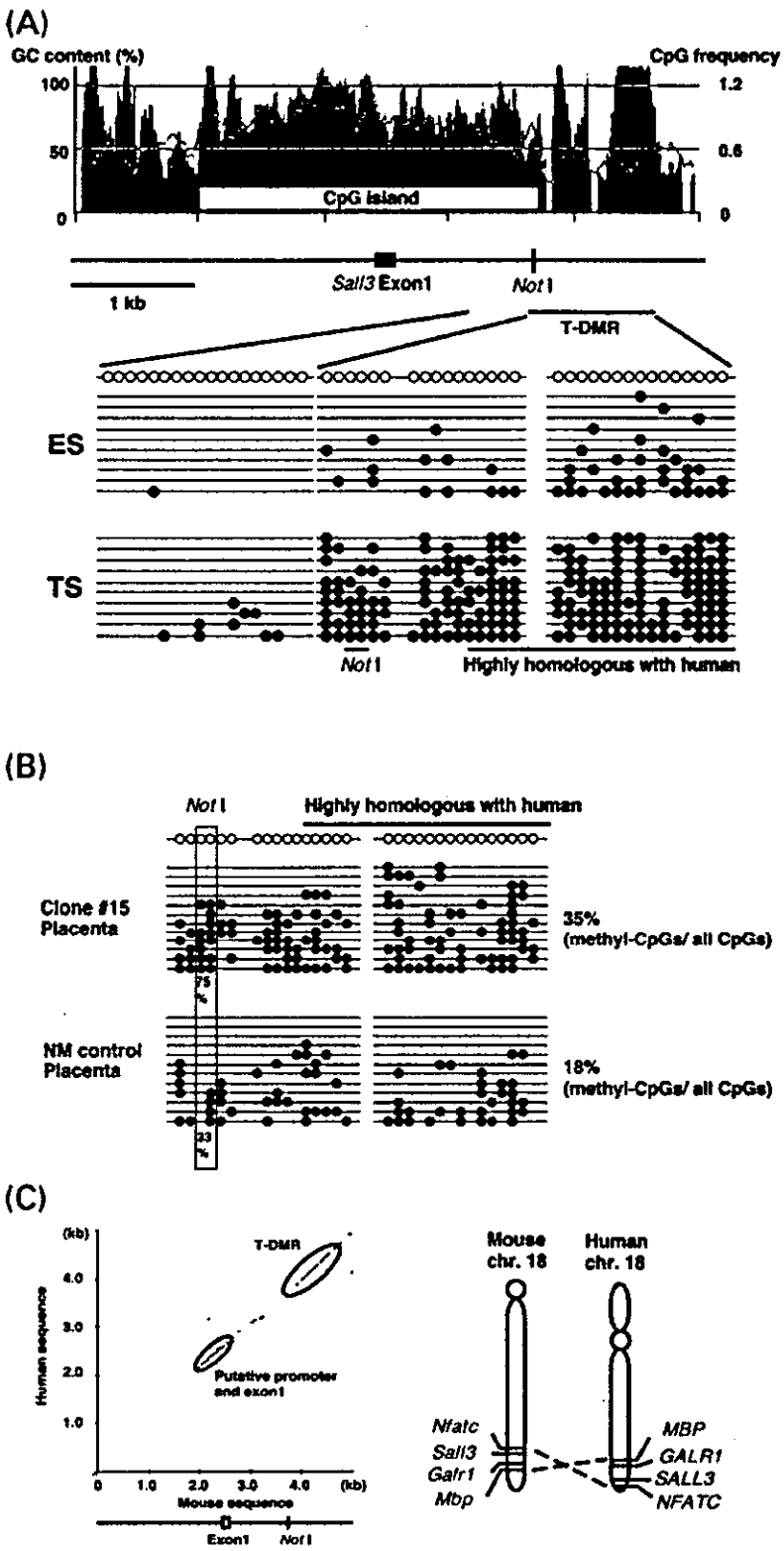

Figure 2 DNA methylation status of T-DMR at the *Sall3* locus in the placenta of cloned mouse. (A) Genomic structure of a 5 kb region that includes *Sall3* exon1, the CpG island, T-DMR and the trophoblast-specifically methylated *Not*I site. Moving averages of GC content (jagged line) and CpG frequency (black bar) are plotted on the graph. Below the graph are marked the *Sall3* exon1 (closed box) and the differentially methylated *Not*I site. The CpG island was formulated by an average GC content greater than 50% and that of CpG frequency greater than 0.6 (Gardiner-Garden & Frommer 1987). Both *Sall3* exon 1 and the trophoblast-specifically methylated *Not*I site are within the CpG island. Methylation status around the differentially methylated *Not*I site in ES and TS cells is shown below the genomic structure of the *Sall3* locus. The CpG sites analysed by sodium bisulfite sequencing are shown as open circles at the very top. Comparison of the methylation status between ES and TS cells indicated that the *Sall3* T-DMR included the differentially methylated *Not*I site and the region highly homologous with human sequence. Each line represents one DNA fragment sequenced. Only methylated CpGs are shown as closed circles. (B) Aberrant hypermethylation throughout the T-DMR in the placenta of a cloned mouse. There are 31 CpGs within the *Sall3* T-DMR, and the CpG sites are shown as open circles at the very top. The positions of two CpGs affecting *Not*I digestion are marked with a box, and their methylation rates are shown by percentage. The overall percentage of methylated CpGs is shown in the right side (methyl-CpGs/all CpGs). In cloned mouse #15, aberrant hypermethylation occurred in the region highly homologous with human sequence. (C) Genomic sequence conservation at and around the *Sall3* locus in human and mouse. (Left panel) Comparison of the nucleotide sequences of the mouse and human *Sall3/SALL3* 5′ region. Within the 5 kb orthologous regions, nucleotide sequences of a putative promoter with exon1 and T-DMR are conserved. (Right panel) Gene map of the telomeric region of mouse and human chromosome 18. The order of genes in this region is conserved in the mouse and in the human but in the reversed order.

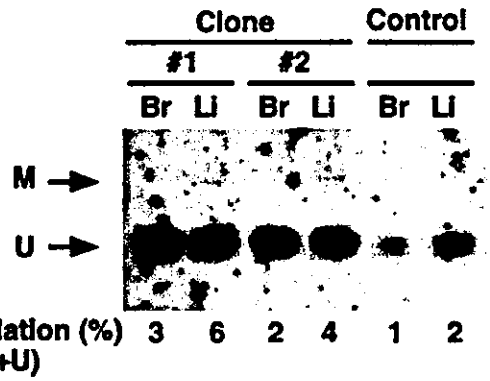

Figure 3 Methylation status at the *Sall3* locus in the brain and liver of cloned fetuses. Methylation status of the *Not*I site in foetal brain (Br) and liver (Li) of cloned and control fetuses were analysed under the same conditions as in Figure 1. Cloned mouse fetuses #1 and #2 are from the same B6D2F1 conceptuses analysed in Figure 1. M and U indicate methylated and unmethylated bands, respectively. The *Sall3* locus is barely methylated both in cloned and control fetuses.

inherited human diseases (OMIM #159430, 600377 and 600489) (Fig. 2C). Among these genes, *NFATC* is suggested to play a role in human placenta (Xia *et al.* 2002). In the case of the *Igf2* gene, the differentially methylated regulatory region is about 90 kb from the transcription start site (Wolffe 2000). Future study is necessary to know the role of the DNA methylation of the *Sall3* T-DMR in the regulation of *MBP*, *CALR1* and *NFATC*. Based on the present study, however, it is clear that the epigenetic abnormality always associates with cloned mice. Taken together, human and mouse orthologous locus including the *SALL3/Sall3* gene may be a region that is genetically and epigenetically instable. Careful examination of epigenetic errors in cloned embryos and fetuses will be needed before somatic nuclear transfer technology is applied to human therapeutics including the production of human embryonic stem cells.

Mouse interspecific hybrids have been reported to show a hypertrophic placental phenotype quite similar to that of cloned placentas (Zechner *et al.* 1996). As found in cloned placentas, these interspecific placentas also exhibited a wide range of placental weight, enlarged spongiotrophoblast layer, increased incidence of glycogen cell differentiation and obscure borders at spongiotrophoblast and labyrinth layers (Zechner *et al.* 1996; Tanaka *et al.* 2001). Since the methylation rate of the *Sall3* T-DMR correlated with the typical placental phenotype (placentomegaly) in cloned mice, it will be interesting to investigate DNA methylation status of the *Sall3* locus in the interspecific hybrid mice.

The production rate of cloned animals is low. Only 2–3% or less, of all reconstituted oocytes, develop into live offspring (Solter 2000; Renard *et al.* 2002; Wilmut *et al.* 2002). Most embryos/fetuses die during development, and improper placental development may be, in part, responsible for this. Establishment of cell- and tissue-specific DNA methylation is important for normal embryonic development (Bird 2002; Li 2002; Shiota & Yanagimachi 2002). Therefore, genomic loci frequently associated with the epigenetic error have been explored in the cloned animals. The finding of the *Sall3* locus showing frequent abnormal DNA methylation is crucial. From the data, we concluded that there is a genomic locus highly susceptible to epigenetic error caused by nuclear transfer.

Experimental procedures

Animals

Placentas, brains and livers of cloned and control fetuses at 19.5 dpc were collected and analysed for DNA methylation. One term placenta of naturally mated mouse was mechanically dissected into the junctional and labyrinth zones after removal of the embryo. Donor cells for cloning were adult cumulus cells (Wakayama *et al.* 1998), adult tail tip fibroblast (Wakayama & Yanagimachi 1999) and foetal fibroblast (Ogura *et al.* 2000b). Control fetuses were obtained by natural mating, *in vitro* fertilization (Toyoda *et al.* 1971) or intracytoplasmic sperm injection (Kimura & Yanagimachi 1995). Strains of males and females used for the production of fetuses are described in figure legends.

Database search and RLGS spot cloning

DNA of an RLGS spot showing aberrant methylation in one cloned mouse (spot 8 in Ohgane *et al.* 2001) was purified by the *Not*I trapper method as described elsewhere (Ohgane *et al.* 1998, 2002). The purified DNA was initially ligated into the *Not*I and *Pst*I sites of pBluescript II (Stratagene, CA). The inserted fragments were amplified by PCR with the M4-RV primer set and cloned into the pGEM-T vector (Promega, WI). Cloned DNA was sequenced by using a Shimadzu autosequencer system (Shimadzu, Kyoto, Japan) following the manufacturer's instructions. The nucleotide sequence obtained from spot DNA cloning was compared with NCBI (http://www.ncbi.nlm.nih.gov) and Ensemble (http://www.ensembl.org) mouse and human genome sequence databases by the BLAST search program. Human genes on chromosome 18 responsible for inherited diseases were ascertained by searching the OMIM database (http://www.ncbi.nlm.nih.gov/entrez/query.fcgi?db = OMIM).

Southern blotting

Genomic DNAs (5 μg each) from cloned and control mouse tissues (placenta, brain and liver) were double-digested with *Not*I and *Pst*I, and separated on a 1.4% agarose gel followed by blotting

on to nylon membrane. A probe specific to spot 8 (the *Sall3* locus) sequence was labelled with a DIG-dUTP using a random primer labelling kit (Roche Diagnostics, Mannheim, Germany). Hybridization and washing were performed under stringent conditions as described elsewhere (Hirosawa *et al.* 1994). Signals were detected with a DIG luminescent nucleotide detection kit (Roche Diagnostics) containing alkaline phosphatase (AP)-conjugated anti-DIG antibody and AP substrate, and visualized on X-ray film (Fuji Film, Tokyo, Japan).

Statistical analysis

The intensities of the methylated and unmethylated bands were measured by NIH image software provided by the National Institutes of Health (ftp://rsbweb.nih.gov/pub/nih-image/nih-image161_fat.hqx). Methylation rate of the *Not*I site of the *Sall3* locus was calculated by the formula: (intensity of methylated band)/(intensity of methylated band) + (intensity of unmethylated band) and presented by mean ± standard deviation. The difference in methylation rate between cloned and control mice was evaluated by the independent Student's *t*-test. The relationship between placental weight and the *Sall3* methylation rate of cloned placentas was tested with Pearson's correlation coefficient, and its *P*-value was evaluated from the coefficient *t*-value.

Bisulfite sequencing

Bisulfite sequencing was performed following previously reported procedure (Imamura *et al.* 2001). In brief, 5 μg each of *Eco*RI-digested genomic DNA were modified with sodium metabisulfite, and one-tenth of each modified DNA was amplified with AmpliTaq Gold (Perkin Elmer, Norwalk, CT, USA) and the following primer sets: BisF1, 5′-GGGAAGTAAATGTTTTTT-GGTT-3′; *Bis*R1, 5′-AACTAACTAAAAAAACTCTATATC-3′; BisF2, 5′-GTTAGGGTTTTTTTAGGGTATTAGT-3′; BisR2, 5′-CCCTAATCTACCCAACATATACAAA-3′; BisF3, 5′-GATTAAATGAATGGATTTATTTTTGT-3′; and BisR3, 5′-ATTAACTATCTAAAATTTTCAACAC-3′. Amplified fragments were cloned into pGEM-T vector (Promega), and 10 or 12 independent clones for each primer set were sequenced to determine methylation status.

Real time PCR

Real time genomic PCR was performed using the ABI PRISM 7900 HT Sequence Detection System (Applied Biosystems, CA) following the manufacturer's instructions. Placental genomic DNAs (40 ng), with or without *Not*I-digestion (methylated DNA or total DNA, respectively) were analysed by real time PCR using F5 (5′-TACCAGCACGGAGGCCGAGGA-3′) and R3 (5′-GATCATAAAAAGTTGGCTTTTAAGG-3′) primer pair flanking the differentially methylated *Not*I site. TaqMan Rodent GAPDH Control Reagent (Applied Biosystems) was used for normalization of the template DNA amount. Methylation degree of the *Not*I site was calculated by the formula: (quantity of methylated DNA)/(quantity of total DNA).

Acknowledgements

We thank Dr Steven Ward for reading the original manuscript and valuable suggestions and Dr Jody Haigh for helpful comments. We also thank Ms. Naoko Sato, Mr Masahiro Kujiraoka, Mr Tetsuya Abe and Mr Stephen Black for their help. This work was supported by the Program for Promotion of Basic Research Activities for Innovative Biosciences and the Grant-in-aid for Scientific Research, Ministry of Education, Culture, Sports, Science and Technology, Japan (11794010) (K.S.), the Harold Castle Foundation and the Victoria and Geist Foundation (R.Y.).

References

Bird, A. (2002) DNA methylation patterns and epigenetic memory. *Genes Dev.* **16**, 6–21.

Bourc'his, D., Le Bourhis, D., Patin, D., *et al.* (2001) Delayed and incomplete reprogramming of chromosome methylation patterns in bovine cloned embryos. *Curr. Biol.* **11**, 1542–1546.

Cross, J.C., Werb, Z. & Fisher, S.J. (1994) Implantation and the placenta: key pieces of the development puzzle. *Science* **266**, 1508–1518.

Doherty, A.S., Mann, M.R.W., Tremblay, K.D., Bartolomei, M.S. & Schultz, R.M. (2000) Differential effect of culture on imprinted H19 expression in the preimplantation mouse embryo. *Biol. Reprod.* **62**, 1526–1535.

Gardiner-Garden, M. & Frommer, M. (1987) CpG islands in vertebrate genomes. *J. Mol. Biol.* **196**, 261–282.

Hill, J.R., Burghardt, R.C., Jones, K., *et al.* (2000) Evidence for placental abnormality as the major cause of mortality in first-trimester somatic cell cloned bovine fetuses. *Biol. Reprod.* **63**, 1787–1794.

Hirosawa, M., Miura, R., Min, K.S., Hattori, N., Shiota, K. & Ogawa, T. (1994) A cDNA encoding a new member of the rat placental lactogen family, PL-I mosaic (PL-Im). *Endocr. J.* **41**, 387–397.

Humpherys, D., Eggan, K., Akutsu, H., *et al.* (2001) Epigenetic instability in ES cells and cloned mice. *Science* **293**, 95–97.

Humpherys, D., Eggan, K., Akutsu, H., *et al.* (2002) Abnormal gene expression in cloned mice derived from embryonic stem cell and cumulus cell nuclei. *Proc. Natl. Acad. Sci. USA* **99**, 12889–12894.

Imamura, T., Ohgane, J., Ito, S., *et al.* (2001) CpG island of rat sphingosine kinase-1 gene: tissue-dependent DNA methylation status and multiple alternative first exons. *Genomics* **76**, 117–125.

Issa, J.P., Ottaviano, Y.L., Celano, P., Hamilton, S.R., Davidson, N.E. & Baylin, S.B. (1994) Methylation of the oestrogen receptor CpG island links ageing and neoplasia in human colon. *Nature Genet.* **7**, 536–540.

Jones, P.L., Veenstra, G.J., Wade, P.A., *et al.* (1998) Methylated DNA and MeCP2 recruit histone deacetylase to repress transcription. *Nature Genet.* **19**, 187–191.

Kang, Y.K., Koo, D.B., Park, J.S., *et al.* (2001) Aberrant methylation of donor genome in cloned bovine embryos. *Nature Genet.* **28**, 173–177.

Kang, Y.K., Park, J.S., Koo, D.B., *et al.* (2002) Limited demethylation leaves mosaic-type methylation states in cloned bovine pre-implantation embryos. *EMBO J.* **21**, 1092–1100.

Kimura, Y. & Yanagimachi, R. (1995) Intracytoplasmic sperm injection in the mouse. *Biol. Reprod.* **52**, 709–720.

Kohlhase, J., Hausmann, S., Stojmenovic, G., *et al.* (1999) SALL3, a new member of the human spalt-like gene family, maps to 18q23. *Genomics* **62**, 216–222.

Lanza, R.P., Cibelli, J.B., Blackwell, C., *et al.* (2000) Extension of cell life-span and telomere length in animals cloned from senescent somatic cells. *Science* **288**, 665–669.

Li, E. (2002) Chromatin modification and epigenetic reprogramming in mammalian development. *Nature Rev. Genet.* **3**, 662–673.

Norris, D.P., Brockdorff, N. & Rastan, S. (1991) Methylation status of CpG-rich islands on active and inactive mouse X chromosomes. *Mamm. Genome* **1**, 78–83.

Ogonuki, N., Inoue, K., Yamamoto, Y., *et al.* (2002) Early death of mice cloned from somatic cells. *Nature Genet.* **30**, 253–254.

Ogura, A., Inoue, K., Ogonuki, N., *et al.* (2000a) Production of male cloned mice from fresh, cultured, and cryopreserved immature Sertoli cells. *Biol. Reprod.* **62**, 1579–1584.

Ogura, A., Inoue, K., Takano, K., Wakayama, T. & Yanagimachi, R. (2000b) Birth of mice after nuclear transfer by electrofusion using tail tip cells. *Mol. Reprod. Dev.* **57**, 55–59.

Ohgane, J., Aikawa, J., Ogura, A., Hattori, N., Ogawa, T. & Shiota, K. (1998) Analysis of CpG islands of trophoblast giant cells by restriction landmark genomic scanning. *Dev. Genet.* **22**, 132–140.

Ohgane, J., Hattori, N., Oda, M., Tanaka, S. & Shiota, K. (2002) Differentiation of trophoblast lineage is associated with DNA methylation and demethylation. *Biochem. Biophys. Res. Commun.* **290**, 701–706.

Ohgane, J., Wakayama, T., Kogo, Y., *et al.* (2001) DNA methylation variation in cloned mice. *Genesis* **30**, 45–50.

Ott, T., Kaestner, K.H., Monaghan, A.P. & Schutz, G. (1996) The mouse homolog of the region specific homeotic gene spalt of Drosophila is expressed in the developing nervous system and in mesoderm-derived structures. *Mech. Dev.* **56**, 117–128.

Renard, J.P., Zhou, Q., LeBourhis, D., *et al.* (2002) Nuclear transfer technologies: between successes and doubts. *Theriogenology* **57**, 203–222.

Santos, F., Hendrich, B., Reik, W. & Dean, W. (2002) Dynamic reprogramming of DNA methylation in the early mouse embryo. *Dev. Biol.* **241**, 172–182.

Schulz, W.A., Elo, J.P., Florl, A.R., *et al.* (2002) Genomewide DNA hypomethylation is associated with alterations on chromosome 8 in prostate carcinoma. *Gene Chromosome Canc.* **35**, 58–65.

Shiota, K., Kogo, Y., Ohgane, J., *et al.* (2002) Epigenetic marks by DNA methylation specific to stem, germ and somatic cells in mice. *Genes Cells* **7**, 961–969.

Shiota, K. & Yanagimachi, R. (2002) Epigenetics by DNA methylation for development of normal and cloned animals. *Differentiation* **69**, 162–166.

Solter, D. (2000) Mammalian cloning: advances and limitations. *Nature Rev. Genet.* **1**, 199–207.

Stoger, R., Kubicka, P., Liu, C.G., *et al.* (1993) Maternal-specific methylation of the imprinted mouse Igf2r locus identifies the expressed locus as carrying the imprinting signal. *Cell* **73**, 61–71.

Suemizu, H., Aiba, K., Yoshikawa, T., *et al.* (2003) Expression profiling of placentomegaly associated with nuclear transplantation of mouse ES cells. *Dev. Biol.* **253**, 36–53.

Takizawa, T., Nakashima, K., Namihira, M., *et al.* (2001) DNA methylation is a critical cell-intrinsic determinant of astrocyte differentiation in the fetal brain. *Dev. Cell* **1**, 749–758.

Tamashiro, K.L., Wakayama, T., Blanchard, R.J., Blanchard, D.C. & Yanagimachi, R. (2000) Postnatal growth and behavioral development of mice cloned from adult cumulus cells. *Biol. Reprod.* **63**, 328–334.

Tanaka, S., Oda, M., Toyoshima, Y., *et al.* (2001) Placentomegaly in cloned mouse concepti caused by expansion of the spongiotrophoblast layer. *Biol. Reprod.* **65**, 1813–1821.

Toyoda, Y., Yokoyama, M. & Hoshi, T. (1971) Studies on fertilization of mouse eggs in vitro. *Jpn. Anim. Reprod.* **16**, 147–151.

Wakayama, T., Perry, A.C., Zuccotti, M., Johnson, K.R. & Yanagimachi, R. (1998) Full-term development of mice from enucleated oocytes injected with cumulus cell nuclei. *Nature* **394**, 369–374.

Wakayama, T. & Yanagimachi, R. (1999) Cloning of male mice from adult tail-tip cells. *Nature Genet.* **22**, 127–128.

Wakayama, T. & Yanagimachi, R. (2001) Mouse cloning with nucleus donor cells of different age and type. *Mol. Reprod. Dev.* **58**, 376–383.

Wilmut, I., Beaujean, N., de Sousa, P.A., *et al.* (2002) Somatic cell nuclear transfer. *Nature* **419**, 583–586.

Wolffe, A.P. (2000) Imprinting insulation. *Curr. Biol.* **10**, R463–R465.

Xia, Y., Wen, H.Y. & Kellems, R.E. (2002) Angiotensin II inhibits human trophoblast invasion through AT1 receptor activation. *J. Biol. Chem.* **277**, 24601–24608.

Xue, F., Tian, X.C., Du, F., *et al.* (2002) Aberrant patterns of X chromosome inactivation in bovine clones. *Nature Genet.* **31**, 216–220.

Zechner, U., Reule, M., Orth, A., *et al.* (1996) An X-chromosome linked locus contributes to abnormal placental development in mouse interspecific hybrid. *Nature Genet.* **12**, 398–403.

Received: 27 November 2003
Accepted: 19 December 2003

Cell, Vol. 119, 1001–1012, December 29, 2004, Copyright ©2004 by Cell Press

Generation of Pluripotent Stem Cells from Neonatal Mouse Testis

Mito Kanatsu-Shinohara,[1] Kimiko Inoue,[5] Jiyoung Lee,[6] Momoko Yoshimoto,[4] Narumi Ogonuki,[5] Hiromi Miki,[5] Shiro Baba,[4] Takeo Kato,[4] Yasuhiro Kazuki,[7] Shinya Toyokuni,[2] Megumi Toyoshima,[3] Ohtsura Niwa,[3] Mitsuo Oshimura,[7] Toshio Heike,[4] Tatsutoshi Nakahata,[4] Fumitoshi Ishino,[5] Atsuo Ogura,[5] and Takashi Shinohara[1,8,*]

[1]Horizontal Medical Research Organization
[2]Department of Pathology and Biology of Diseases
Graduate School of Medicine
[3]Radiation Biology Center
Kyoto University
Kyoto 606-8501
[4]Department of Pediatrics
Graduate School of Medicine
Kyoto University
Kyoto 606-8507
[5]The Institute of Physical and Chemical Research
RIKEN
Bioresource Center
Ibaraki 305-0074
[6]Medical Research Institute
Tokyo Medical and Dental University
Tokyo 101-0062
[7]Department of Molecular and Cell Genetics
School of Life Sciences
Faculty of Medicine
Tottori University, Yonago
Tottori 683-8503
Japan

Summary

Although germline cells can form multipotential embryonic stem (ES)/embryonic germ (EG) cells, these cells can be derived only from embryonic tissues, and such multipotent cells have not been available from neonatal gonads. Here we report the successful establishment of ES-like cells from neonatal mouse testis. These ES-like cells were phenotypically similar to ES/EG cells except in their genomic imprinting pattern. They differentiated into various types of somatic cells in vitro under conditions used to induce the differentiation of ES cells and produced teratomas after inoculation into mice. Furthermore, these ES-like cells formed germline chimeras when injected into blastocysts. Thus, the capacity to form multipotent cells persists in neonatal testis. The ability to derive multipotential stem cells from the neonatal testis has important implications for germ cell biology and opens the possibility of using these cells for biotechnology and medicine.

*Correspondence: takashi@mfour.med.kyoto-u.ac.jp
[8]Present address: Department of Molecular Genetics, Graduate School of Medicine, Kyoto University, Kyoto 606-8507, Japan.

Introduction

Germ cells are unique in that they have the capacity to contribute genes to offspring. Although germ cells are highly specialized cells for the generation of gametes, several lines of evidence suggest their multipotentiality. For example, teratomas are tumors containing many kinds of cells and tissues at various stages of maturation, which occur almost exclusively in the gonads (Stevens, 1984). Furthermore, primordial germ cells (PGCs) from embryos between 8.5 and 12.5 days postcoitum (dpc) give rise to pluripotent cells when cultured under appropriate conditions (Resnick et al., 1992; Matsui et al., 1992). These EG cells have differentiation properties similar to ES cells isolated from inner cell mass (Martin, 1981; Evans and Kaufman, 1981). While these observations suggest that the germline lineage retains the ability to generate pluripotent cells, it has not been possible to establish pluripotent cells from normal neonatal gonads (Labosky et al., 1994).

We recently reported the in vitro culture of mouse spermatogonial stem cells (Kanatsu-Shinohara et al., 2003a), the only type of stem cell in the body that transmits genetic information to offspring (Meistrich and van Beek, 1993; de Rooij and Russell, 2000). When neonatal testis cells were cultured in the presence of glial cell line-derived neurotrophic factor (GDNF), leukemia inhibitory factor (LIF), epidermal growth factor (EGF), and basic fibroblast growth factor (bFGF), the germ cells developed uniquely shaped colonies, and the stem cells proliferated logarithmically over a 5 month period. Upon transplantation into the seminiferous tubules of infertile mice, the cultured cells produced normal sperm and offspring, and neither somatic differentiation nor teratoma formation was observed, indicating that the cultured cells were fully committed to the germ cell lineage (Kanatsu-Shinohara et al., 2003a). This was in contrast to ES cells, which produced teratoma after being transferred into seminiferous tubules (Brinster and Avarbock, 1994). Based on these results, we named these cells germline stem (GS) cells to distinguish them from ES or EG cells. Thus, GS cells represent a third method of expanding germline cells, but they are clearly distinct from ES/EG cells in their differentiation capacity.

In this manuscript, we describe the derivation of pluripotent stem cells from the neonatal mouse testis. Neonatal testis cells were cultured in conditions similar to those used for GS cell culture. In addition to the GS cell colonies, colonies indistinguishable from ES cell colonies appeared. This second cell type could be expanded selectively under culture conditions used for ES cells. Although they produced teratomas when transplanted subcutaneously or into the seminiferous tubules of the testis, they participated in normal embryonic development following injection into blastocysts.

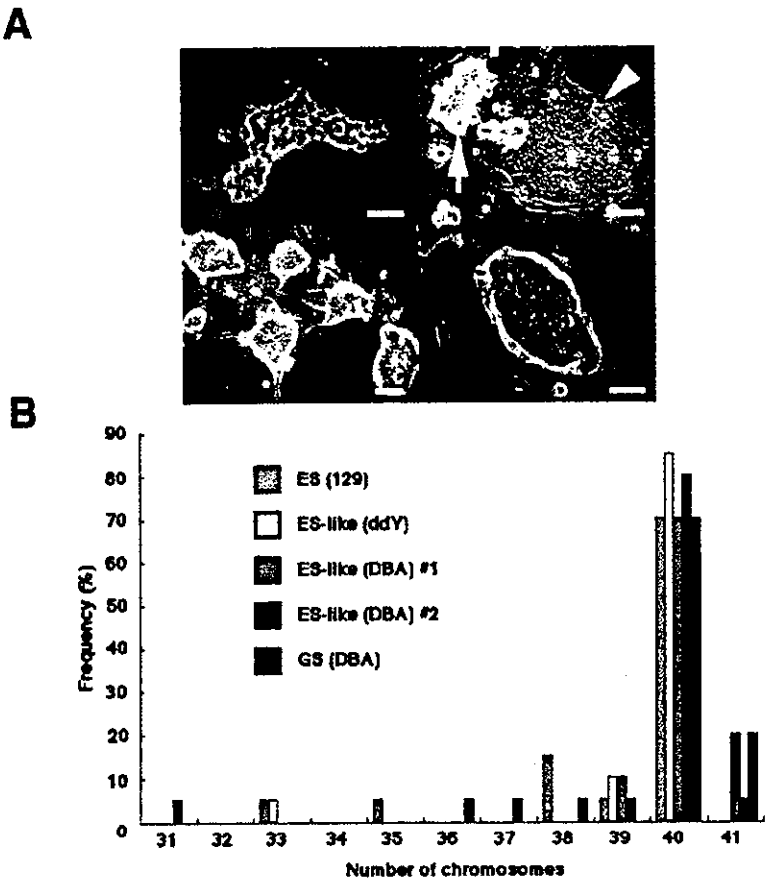

Figure 1. ES-Like Colonies from Neonatal Testis Cells

(A) Morphology of ES-like cells. (Top, left) A typical colony of GS cells. (Top, right) ES-like colony (arrow) and cultured epiblast-like colony (arrowhead), which appeared under GS cell culture conditions, at 40 days after the initiation of culture. (Bottom, left) Established culture of ES-like cells at 50 days. (Bottom, right) A typical colony of ES-like cells at 95 days.

(B) Distribution of metaphase spreads with different chromosome numbers. At least 20 cells were counted. Scale bar, 50 μm.

Results

Development of ES-Like Colonies from Neonatal Testis Cells in the Presence of Growth Factors

When neonatal ddY mouse testis cells were cultured in a primary medium containing GDNF, bFGF, EGF, and LIF, the majority of the colonies that formed had the typical appearance of GS cells, which are characterized by intercellular bridges and a morula-like structure (Figure 1A, top left) (Kanatsu-Shinohara et al., 2003a). However, we occasionally found colonies that were remarkably similar to ES cells or cultured epiblast cells (Figure 1A, top right) (Kanatsu and Nishikawa, 1996). These colonies were more tightly packed and generally appeared within 4–7 weeks after initiation of the culture (~four to seven passages). After these ES cell-like colonies appeared, they outgrew the GS cells and became the dominant population within 2–3 weeks. Although these ES-like colonies generally differentiated to lose their ES cell-like appearance after several passages under GS cell culture conditions, they retained ES-like appearance and could be selectively expanded when cultured in a secondary medium containing 15% fetal calf serum (FCS) and LIF (standard ES cell culture conditions).

After two to three passages, most colonies in the culture consisted of these ES-like colonies (Figure 1A, bottom left), which could be maintained with standard ES cell culture conditions. In contrast, GS cells could not be propagated under these conditions due to the absence of GDNF, an essential growth factor for the self-renewing division of spermatogonial stem cells (Meng et al., 2000). Cytogenetic analysis by quinacrine plus Hoechst 33258 staining showed that the ES-like cells had a normal karyotype (40, XY) in 70%–85% of metaphase spreads (Figure 1B). The morphology of the ES-like cells did not change as long as the cells were maintained in ES cell culture conditions, and they could be propagated in vitro for more than 5 months with 48 passages while maintaining an undifferentiated state (Figure 1A, bottom right). Established cultures were passed at a dilution of 1:3 to 1:6 every 3 days.

These results were reproducible; similar cells were obtained from mice with a different genotype (DBA/2), and ES-like cells were successfully established in four of 21 experiments (19%). The overall frequency of forming ES-like cells was 1 in 1.5×10^7 cells (equivalent to ~35 newborn testes). Significantly, neither GS nor ES-like cells appeared when newborn testis cells were cultured directly in ES culture conditions in at least 20 experiments. Likewise, neither GS nor ES-like cells appeared when neonatal testis cells were cultured in the presence of membrane bound Steel factor (mSCF), LIF, and bFGF (EG cell culture condition) in at least 15 experiments; the addition of GDNF was a prerequisite for the development of both GS and ES-like colonies. In addition, when CD9-selected adult spermatogonial stem cells from 3- to 8-week-old mice were cultured (Kanatsu-Shinohara et al., 2004), GS cells appeared in three of 15

experiments, but no ES-like cells appeared. We also did not observe GS or ES-like cell colonies when male genital ridges from 12.5 dpc embryos were cultured in GS cell medium in 12 experiments.

Development of ES-Like Colonies from GS Cells Derived from p53 Knockout Mice

To determine whether GS cells can convert to ES-like cells, we picked a total of 266 GS cell colonies by micromanipulation at 2 months after culture initiation. These GS cells were transferred to a 96-well plate and expanded for an additional 3 months, but none of them became ES-like cells. Although the result strongly suggested the distinct origin of ES-like cells, it was still possible that the conversion occured at lower frequency. To address this possibility, we used p53 knockout mice (Tsukada et al., 1993), which have a high frequency of testicular teratoma (Lam and Nadeau, 2003). We hypothesized that ES-like cells have a close relationship with teratoma-forming cells and asked whether established GS cells from this strain convert more easily to ES-like cells. GS cells were established from a newborn p53 knockout mouse in an ICR background. The growth speed and morphology of GS cells were indistinguishable from those of wild-type cells, and GDNF was similarly required to obtain GS cells.

Two months after culture, 30–40 GS cell colonies of undifferentiated morphology were picked by micromanipulation, transferred to a 96-well plate, and cultured in GS cell culture medium. Significantly, ES-like cells appeared in these GS cell-derived cultures in two separate experiments within 2 months, and the colonies were morphologically indistinguishable from ES-like colonies from wild-type cells. Interestingly, although ES-like cells never appeared from fully established wild-type GS cells after long-term culture, p53 knockout GS cells produced ES-like cells as long as 6 months after the initiation of culture.

Using p53 knockout mice, we also examined whether GS cells from mature testis can produce ES-like cells. Spermatogonial stem cells were collected from 3- to 8-week-old mice using anti-CD9 antibody and cultured in GS cell medium. GS cells developed in two of three experiments. GS cells of undifferentiated morphology were picked 4–7 days after culture initiation, and the colonies were expanded in vitro on mitomycin C-inactivated mouse embryonic fibroblast (MEF). In total, ES-like cells appeared in two of eight experiments within 4 weeks of culture.

Phenotypic Analysis of ES-Like Cells

To examine the phenotype of the ES-like cells, we established a population from a newborn transgenic mouse line C57BL6/Tg14(act-EGFP-OsbY01) that was bred into the DBA/2 background (designated Green). Since these Green mice express the enhanced green fluorescence protein (EGFP) gene ubiquitously, including in spermatogenic cells (Kanatsu-Shinohara et al., 2003a), cultured cells can be distinguished from feeder cells under excitation with UV light. The ES-like cells comprised a single phenotypic population by flow cytometric analysis of surface antigens (Figure 2A). They were strongly positive for SSEA-1 (ES cell marker) (Solter and Knowles, 1978), EE2 (spermatogonia marker) (Koshimizu et al., 1995), β1- and α6-integrin (GS cell marker) (Kanatsu-Shinohara et al., 2003a), CD9 (ES and GS cell marker) (Kanatsu-Shinohara et al., 2004), and EpCAM (ES and spermatogonia cell marker) (Anderson et al., 1999). The ES-like cells were weakly positive for Forssman antigen (ES cell marker) (Evans and Kaufman, 1981) and c-kit (differentiated spermatogonia marker) (Schrans-Stassen et al., 1999). In contrast, GS cells were completely negative for SSEA-1 and Forssman antigen, confirming that ES-like cells are phenotypically distinct from GS cells. GS cells from p53 knockout mice showed similar expression profile (data not shown). Although we found some expression of Forssman antigen in the neonatal testis cell population before culture, it was expressed by a non-germ cell population, and no SSEA-1-positive cells were found (Figures 2A and 2B). The ES-like cells were also strongly positive for alkaline phosphatase (ALP), which is characteristic of ES and EG cells (Resnick et al., 1992; Matsui et al., 1992) (Figure 2C).

Next, we used the reverse transcriptase-polymerase chain reaction (RT-PCR) to examine several molecules that are specifically expressed in embryonal carcinoma (EC) or ES cells. In addition to Oct-4, Rex-1, and Nanog, which are essential for maintaining undifferentiated ES cells (Pesce and Schöler, 2001; Goolsby et al., 2003; Mitsui et al., 2003; Chambers et al., 2003), the ES-like cells expressed Cripto, ERas, UTF1, Esg-1, and ZFP57 at similar levels to ES cells (Kimura et al., 2001; Takahashi et al., 2003; Okuda et al., 1998; Tanaka et al., 2002; Ahn et al., 2004). GS cells also expressed some of these molecules, but the expression was generally weaker. Significantly, we could not detect expression of Nanog in GS cells, suggesting that they have a different mechanism for self-renewal from that of ES cells (Figure 2D).

Analysis of Genomic Imprinting in ES-Like Cells

To analyze the imprinting pattern of ES-like cells, differentially methylated regions (DMRs) of three paternally imprinted regions (*H19*, *Meg3 IG*, and *Rasgrf1* regions) and two maternally imprinted regions (*Igf2r* and *Peg10* regions) were examined by bisulfite sequencing with two independent cells (Figure 3A). While the paternally imprinted regions were methylated to different degrees, the maternally imprinted regions were rarely methylated in ES-like cells. DMRs in ES cells were generally more methylated than those in ES-like cells, including maternally imprinted regions, and the DMRs of the *H19* region were methylated more extensively than the DMRs of other regions. In contrast, GS cells showed a complete androgenetic imprinting pattern: the complete methylation of both the *H19* and *Meg3 IG* DMRs and demethylation of the *Igf2r* DMR.

Next, we examined the imprint status of GS or ES-like cells from p53 knockout mice. Genomic DNA was isolated from the same cell population at four different time points during the conversion of GS cells into ES-like cells. In these experiments, the imprint status in the DMRs was determined by combined bisulfite restriction analysis (COBRA) (Xiong and Laird, 1997) (Figure 3B). As expected from the analysis of wild-type GS cells, GS

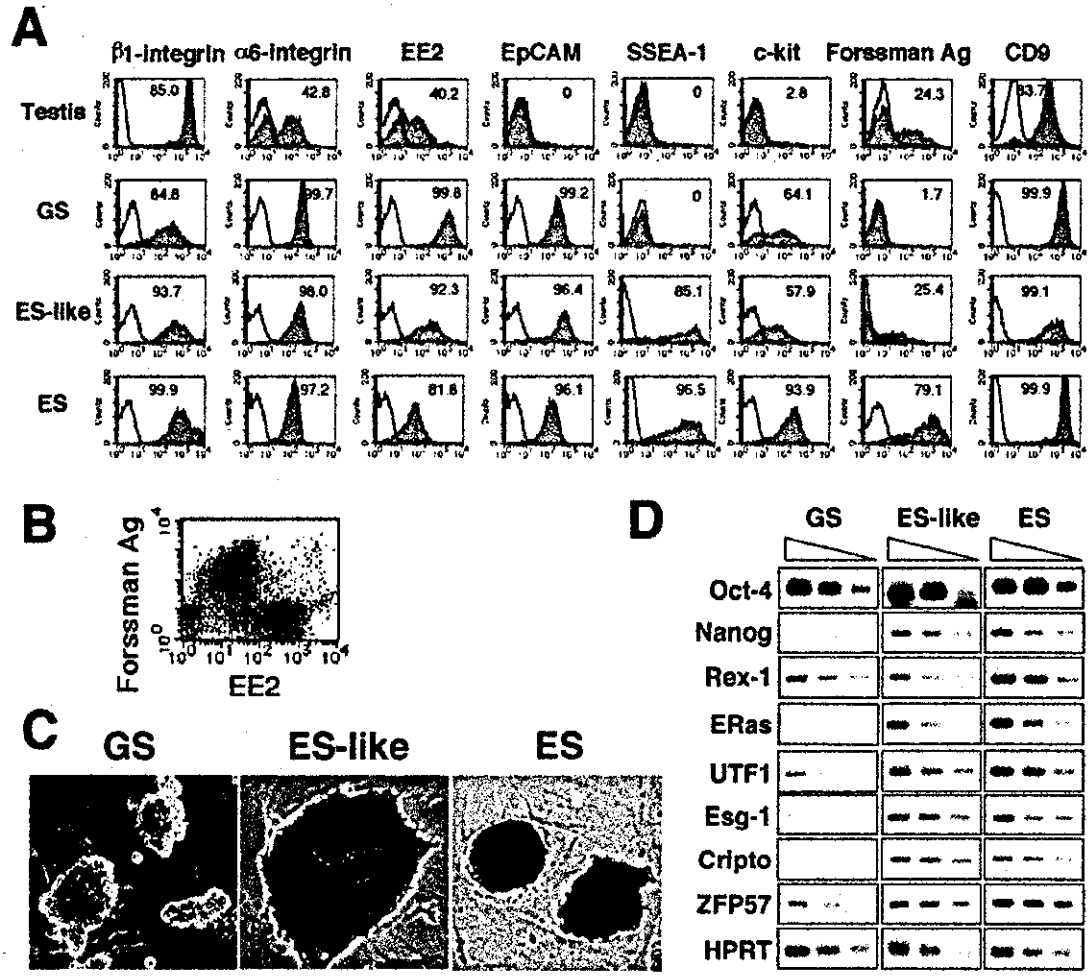

Figure 2. Phenotypic Characterization of ES-Like Cells

(A) Flow cytometric characterization of ES-like cells. Black line, control immunoglobulin; red line, specific antibody.

(B) Double immunostaining of neonatal testis cells by anti-EE2 and anti-Forssman antigen antibodies.

(C) ALP staining. GS cells (left) are weakly positive, whereas ES-like (middle) and ES cells (right) are strongly positive.

(D) RT-PCR analysis. Three-fold serial dilutions of cDNA from GS, ES-like, and ES cells were amplified with specific primers. Scale bar, 200 μm.

cells from p53 KO mice had an androgenetic imprint pattern. However, a loss of methylation in the DMRs of *H19*, *Meg 3/G*, and *Rasgrf1* regions and methylation of the DMRs in the *Igf2r* region were observed immediately after the appearance of ES-like cells. The perturbation of imprint patterns continued even when GS cells disappeared, and only the DMR of the *Peg10* region was intact, 18 days after the appearance of ES-like cells. DMR of *Oct-4* region in ES and ES-like cells were all hypomethylated, which confirms their undifferentiated state (Hattori et al., 2004) (Figure 3C).

Differentiation Potential of ES-Like Cells In Vitro and In Vivo

To determine whether ES-like cells can differentiate into somatic cell lineages, we used methods designed to induce differentiation of ES cells in vitro. ES-like cells were first transferred to an OP9 stromal feeder layer, which can support differentiation of mesodermal cells such as hematopoietic or muscle cells (Nakano et al., 1994; Schroeder et al., 2003). Within 10 days, a variety of cell types were identified including hematopoietic cells, vascular cells, and spontaneously beating myocytes (Figures 4A–4H). Hematopoiesis could also be induced when ES-like cells were cultured in methylcellulose to form embryoid bodies (Figure 4I). When we transferred ES-like cells onto gelatin-coated dishes for the differentiation of neural-lineage cells (Ying et al., 2003), they formed neurons or glial cells (Figures 4J–4L). Dopaminergic neurons were also found, albeit at low frequency (Figure 4M). When we compared the differentiation efficiency using ES cells, ES-like cells produced more glial cells than did ES cells, and there were significantly more vessel or heart muscle cell colonies from ES-like cells. However, ES-like cells could produce all of the expected lineages using protocols for ES cell differentiation (Table 1).

ES-like cells were further examined for their ability to form teratomas in vivo by subcutaneous injection into nude mice. Transplanted cells gave rise to typical teratomas in all recipients (eight of eight) by 4 weeks after transplantation (Figure 4N). The tumors contained deriv-

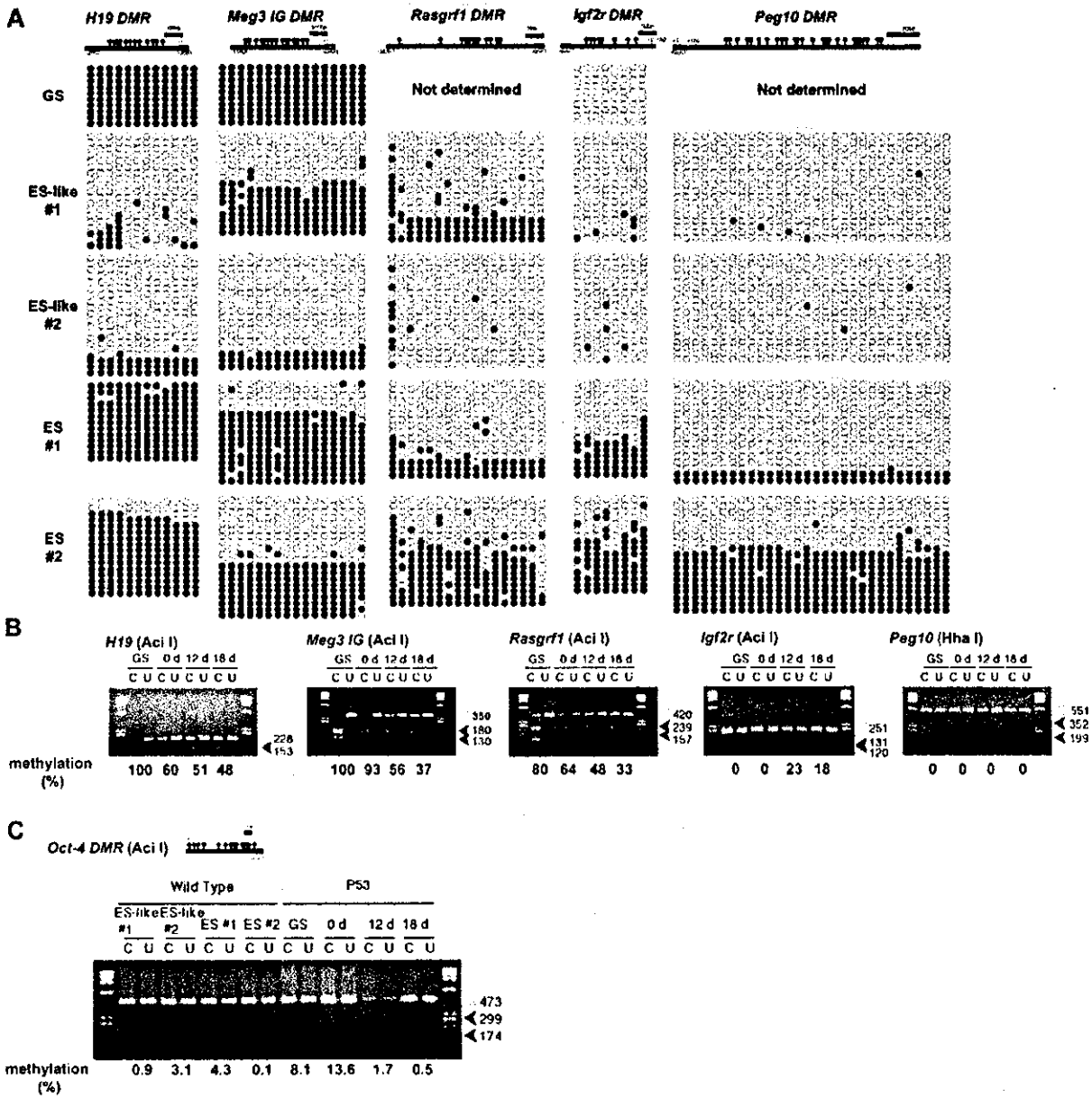

Figure 3. Analysis of Imprinting in ES-Like Cells

(A) DMR methylation of *H19, Meg3 IG, Rasgrf1, Igf2r,* and *Peg10* regions. DNA methylation was analyzed by bisulfite genomic sequencing. Black ovals indicate methylated cytosine-guanine sites (CpGs), and white ovals indicate unmethylated CpGs.

(B) COBRA of GS and ES-like cells from p53 knockout mice. The day when ES-like colonies were found was designated day 0, and cells were collected at the indicated time. In this culture, only ES-like cells were found by day 12.

(C) COBRA of *Oct-4* gene upstream region. Open arrowheads indicate the size of unmethylated DNA. Closed arrowheads indicate the size of methylated DNA. Enzymes used to cleave each locus are indicated in parentheses. U, uncleaved; C, cleaved.

atives of the three embryonic germ layers: squamous cell epithelium, neuroepithelium, and muscle. Similar results were obtained with three different clones or with ES-like cells from p53 knockout mice (eight of eight), and we did not observe a significant histological difference from teratomas derived from ES cells. In contrast, no tumors developed after transplantation of GS cells or fresh testis cells (data not shown).

Since the ES-like cells originated from testis, their ability to differentiate into germline cells was examined using the spermatogonial transplantation technique (Brinster and Zimmermann, 1994). This method allows spermatogonial stem cells to recolonize the empty seminiferous tubules of infertile animals and differentiate into mature sperm. We transplanted the cultured cells into immune-suppressed immature W mice (Kanatsu-Shinohara et al., 2003b). These mice are congenitally infertile and have no differentiating germ cells (Brinster and Zimmermann, 1994). One month after transplantation, all recipient animals (ten of ten) developed teratomas in

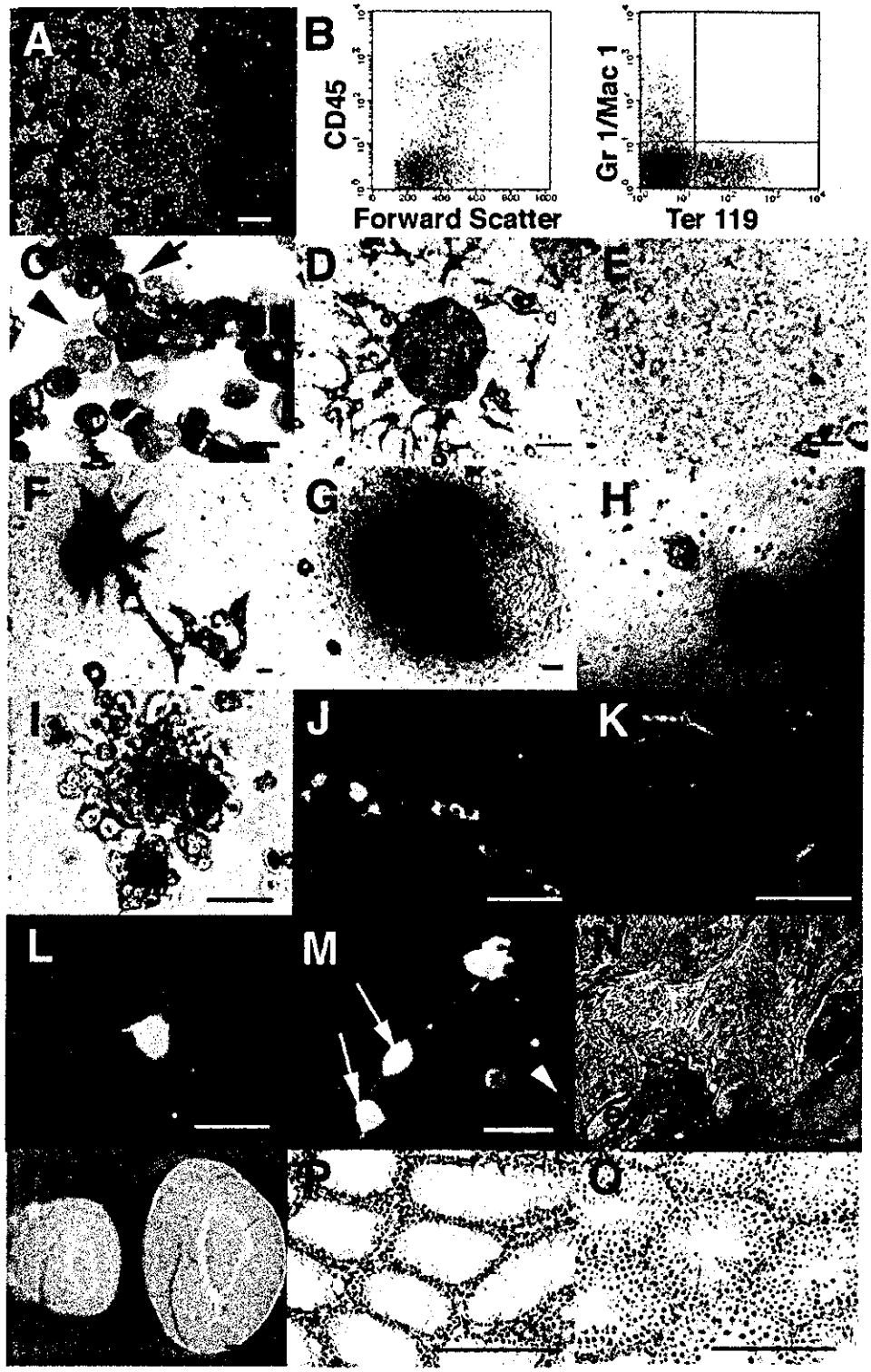

Figure 4. In Vitro and In Vivo Differentiation of ES-Like Cells

(A–H) Differentiation on OP9 cells. (A) Cobblestone formation on day 8. (B) CD45-positive hematopoietic cell development on day 7 after coculture (left). In this cell population, Gr1-positive granulocytes, Mac1-positive macrophages, or Ter119-positive erythrocytes were found (right). (C) May-Giemsa staining of harvested cells. Myeloid progenitor (arrowhead) and erythroblast (arrow) were observed. (D and E) Vascular cell differentiation. Flk-1-positive cells were sorted on day 4 after coculture, and CD31-positive (D) or VE-cadherin-positive (E) vascular cells appeared at 6 days after cell sorting. (F–H) Heart muscle differentiation. The Flk-1-positive cells were differentiated into MF20-positive (F) or cTn-I-positive (G) heart muscle at 6 days after sorting. (H) ANP-positive (blue) atrial muscle and MLC2v-positive (brown) ventricular muscle.
(I) Erythroid cells that developed from embryoid body in methylcellulose at 8 days after culture. Note the red color of the cells.
(J–M) Neuronal cell differentiation on gelatin-coated plates. Tuj-positive neurons (J) on day 5, GFAP-positive astrocytes (K) and MBP-positive

Table 1. In Vitro Differentiation of ES-Like Cells from Testis

	Hematopoiesis[a,b]			Vasculogenesis[a,c]		Neurogenesis[d]		
Cell type	Increase in cell number (fold)	Granulocyte/ Macrophage (%)	Erythrocyte[e] (%)	Vessel[e]	Heart[e]	Neuron[e]	Astrocyte[e]	Oligodendrocyte[e]
ES-like	116.7 ± 15.4	7.6 ± 0.2	19.9 ± 0.7	111.5 ± 12.0	8.0 ± 4.5	126.7 ± 14.4	34.6 ± 4.4	4.6 ± 2.5
ES cell	102.3 ± 11.6	7.6 ± 0.4	24.7 ± 0.9	49.0 ± 9.2	3.8 ± 2.0	162.2 ± 14.5	10.5 ± 3.3	0.2 ± 0.1

Values are mean ± SEM. Results from at least three experiments. ES cells were derived from 129 mice, whereas ES-like cells were derived from DBA/2 mice.

[a] Flk-1-positive cells (5×10^5) were sorted 4 days after coculture and replated on OP9 feeder in a 24-well plate.

[b] Cells were recovered 7 days after sorting and analyzed by flow cytometry. Erythrocytes, macrophages, and granulocytes were identified by anti-Ter119, anti-Mac1, and anti-Gr1 antibodies, respectively.

[c] Numbers of positive cells in each well, 8 days after sorting. Vascular cells were determined by the uptake of DiI-acetylated low-density lipoprotein. Heart muscle colonies were identified by counting beating colonies.

[d] Cells (2.5×10^4) were plated on gelatin in a 48-well plate, and numbers of positive cells per cm^2 were determined by immunocytochemistry 5 (neuron) or 7 (astrocytes or oligodendrocytes) days after plating. Neurons were identified by anti-Tuj antibody, whereas astrocytes and oligodendrocytes were identified by anti-GFAP or anti-MBP antibodies, respectively. Dopaminergic neurons were produced ~10 cells per well.

[e] Statistically significant by Student's t test ($p < 0.05$).

the testis. The seminiferous tubules were disorganized, and no sign of spermatogenesis was found in histological sections. The cell composition found in the teratomas was similar to that of tumors that developed after subcutaneous injection (data not shown). In contrast, both wild-type and p53 KO GS cells produced normal spermatogenesis when transplanted into the seminiferous tubules (Figures 4O–4Q).

Contribution of ES-Like Cells to Normal Embryonic Development after Blastocyst Injection

Finally, we microinjected ES-like cells into blastocysts to examine whether they can contribute to chimeras in vivo. Five to fifteen cells were injected into C57BL/6 blastocysts. The ratio of euploid cells, which significantly influences the rate of chimerism or germline transmission (Longo et al., 1997; Liu et al., 1997), was 70% at the time of injection.

Some of the recipient animals were analyzed at 12.5 dpc to look for chimerism, and others were allowed to develop to term. Chimerism was observed in 25% (three of 12) of the 12.5 dpc embryos (Figure 5A) and in 36% (13 of 36) of the newborn animals (Figure 5B), as judged by the expression of EGFP observable under UV illumination. Chimerism was also confirmed by the coat color at mature stage (Figure 5C). We found six dead fetuses that showed EGFP expression, and some embryos were partially or completely absorbed. The pattern of contribution was similar at both stages analyzed; EGFP-positive donor cells were found in the central nervous system, liver, heart, lung, somites, intestine, and other tissues, including the yolk sac and chorionic membrane of the placenta (Figures 5D–5I).

Since donor cells were also found in the testis of a chimeric animal at 6 weeks of age (Figure 5J), we performed microinsemination to obtain offspring. Round spermatids were collected and microinjected into C57BL/6 × DBA/2 (BDF1) oocytes. Of 81 cultured embryos, 64 (79%) developed into 2-cells and were transferred into five psudopregnant females. Eighteen (22%) embryos were implanted, and one of the two offspring from a recipient mouse showed EGFP fluorescence, indicating the donor origin (Figure 5K). Interestingly, while control ES cells showed wide contribution to embryos, no donor cell contribution was observed in experiments using GS cells (Table 2).

To determine the full developmental potential of ES-like cells, we used tetraploid complementation technique (Nagy et al., 1993). This technique allows the production of live animals that consist entirely of donor ES cells. A total of 92 tetraploid embryos were created by electrofusion, aggregated with ES-like cells, and transferred to pseudopregnant ICR females. When some of the recipient animals were sacrificed at 10.5 dpc, we found one normal-looking fetus and several resorptions with normal placentas. The fetus showed some growth retardation but clearly expressed the EGFP gene throughout its body, including the yolk sac (Figure 5L), indicating that it was derived from donor ES-like cells. However, none of the pseudopregnant mothers sired live offspring from both ES-like and ES cells.

Discussion

The results of our experiments revealed the presence of multipotential stem cells in the neonatal testis. Although some cases of the "stem cell plasticity" phenomenon

oligodendrocytes (L) on day 7 after induction. TH and Tuj-double positive dopaminergic neurons (arrow) appeared among Tuj-positive neurons (arrowhead) (M).

(N) Section of a teratoma under the skin. The tumors contained a variety of differentiated cell types, including muscle (m), neural (n), and epithelial (e) tissues.

(O–Q) Spermatogenesis from p53 knockout GS cells. (O) A macroscopic comparison of untransplanted (left) and transplanted (right) recipient testes. Note the increased size of the transplanted testis. (P and Q) Histological appearance of the untransplanted (P) and transplanted (Q) W testes. Note the normal appearance of spermatogenesis (Q). Color staining: Cy3, red (J–M); Alexa Fluor 488, green (M). Scale bar, 50 μm (A, D–H, J, K, and M), 20 μm (C and L), 200 μm (N, P, and Q), 1 mm (O).

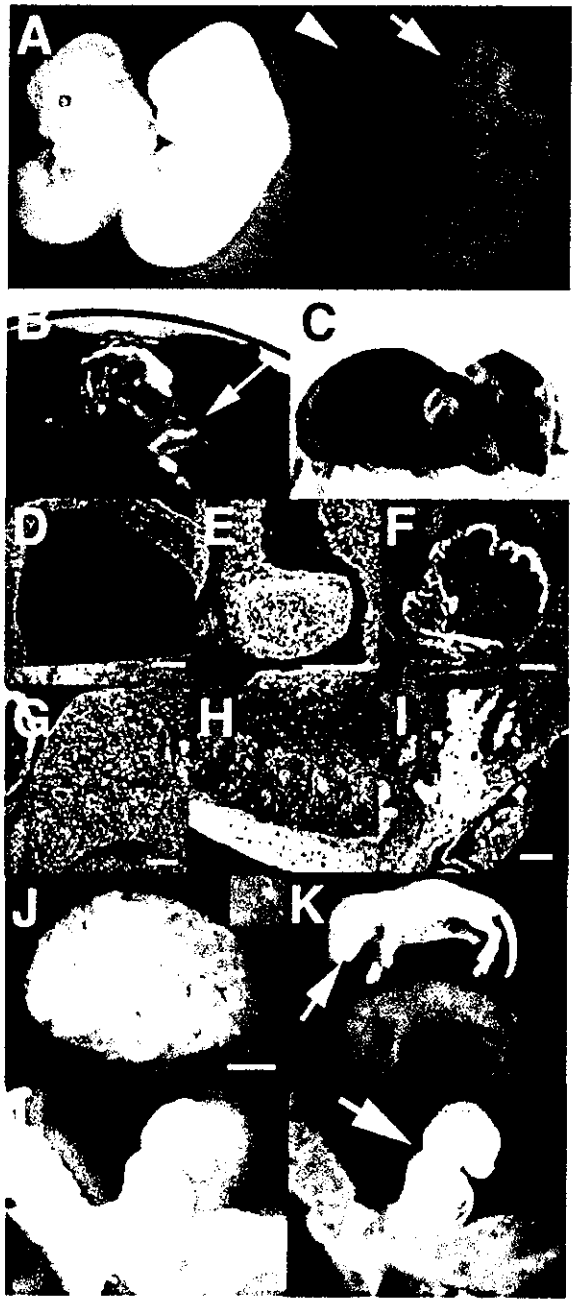

Figure 5. Production of Chimeric Animals

(A) A 12.5 dpc chimeric embryo (arrow) showing fluorescence under UV light. No fluorescence was observed in a control embryo (arrowhead).

(B) A newborn chimeric animal (arrow) showing fluorescence.

(C) Mature chimeric animals. Note the donor cell-derived coat color (cinnamon).

(D–I) Parasagittal section of a 12.5 dpc chimeric embryo. Fluorescence was observed in the brain (D), intestine (E), heart (F), liver (G), lower spinal cord (H), and placenta (I).

(J) A testis from a chimeric mouse showing fluorescence. EGFP expression was observed in some germ cells in the testis cell suspension (inset).

(K) Offspring derived from a chimera. One of the offspring showed fluorescence, confirming the donor origin (arrow).

(L) A 10.5 dpc embryo (arrow) and yolk sac produced from an aggregation of ES-like cells with tetraploid embryo showing fluorescence. No fluorescence was observed in the placenta (arrowhead). Counterstained with propidium iodide (PI) (D–I). Color staining: EGFP, green (A, B, and D–L); PI, red (D–I). Scale bar, 100 μm (D–I), 1 mm (J).

have been attributed to cell fusion (Wagers and Weissman, 2004), our case cannot be explained by the same mechanism because the ES-like cells formed teratomas after subcutaneous transplantation. These ES-like cells from the testis can be considered the neonatal counterparts of ES/EG cells. The result was unexpected, since PGCs become resistant to experimental teratocarcinogenesis or EG cell formation after 13.5 dpc (Stevens, 1984; Labosky et al., 1994). To our knowledge, EG cells are the only example of the isolation of multipotent stem cells from primary germ cells (Resnick et al., 1992; Matsui et al., 1992). EG cells were derived from primary germ cells harvested from 8.5 to 12.5 dpc fetuses and cultured in vitro with a mixture of mSCF, LIF, and bFGF. However, pluripotent cells could not be isolated from neonatal germ cells using the same culture conditions (Labosky et al., 1994), except when cells from teratomas were used (Robertson and Bradley, 1986). ES-like cells are unlikely to be derived from teratoma cells for two reasons. First, the frequency of derivation of ES-like cells in our study was significantly higher than the negligible rate of spontaneous teratoma formation in strains other than 129 and A/He mice (one teratoma out of 11,292 males in 129 hybrid backgrounds) (Stevens and Mackensen, 1961). Second, growth factor supplementation was essential for the establishment of ES-like cells. In fact, few EC cell lines have been obtained from spontaneously occurring teratocarcinomas (Robertson and Bradley, 1986). These findings strongly suggest that the ability to become multipotent stem cells persists in neonatal testis. Based on the results reported here, we propose to name these ES-like cells multipotent germline stem cells, or mGS cells, to distinguish them from GS cells, which can differentiate only into germline cells (Kanatsu-Shinohara et al., 2003a).

An important question that arises from this study is the origin of mGS cells. One possibility is that they appear independently from GS cells and originate from a population of undifferentiated pluripotent cells that persist in the testis from the fetal stage. Although EG cells have been established from ~12.5 dpc PGCs (Matsui et al., 1992; Labosky et al., 1994), cells with similar characteristics might remain in neonatal testis and produce ES-like cells. Indeed, the results of the imprinting analysis of wild-type mGS cells suggest a distinct origin for mGS cells. In male germ cells, genomic imprinting is erased during the fetal stage, and male-specific imprinting begins to be acquired around birth in prospermatogonia and is completed after birth (Davis et al., 1999, 2000; Kafri et al., 1992). While GS cells had a typical androgenetic imprinting pattern, the imprinting pattern of mGS cells clearly differed from those of androgenetic germ cells or somatic cells, which suggested that mGS cells originate from partially androgenetic germ cells that have undergone imprint erasure.

Another possibility is that mGS cells are derived from spermatogonial stem cells and that the ability to become multipotential cells may be one of the general character-

Table 2. Contribution of ES-Like Cells to Embryonic Development

Type of Cells	Number of Embryos Transferred	Number of Recipients	Number of Pups Born[a]	Number of Live Pups[b]	Chimera (%)	
					Male	Female
ES-like	193	11	54	36	9/22 (41)	4/14 (29)
ES	91	14	14	4	2/2 (100)	2/2 (100)
GS	124	7	28	16	0/8 (0)	0/8 (0)
4n rescue ES-like	92	4	0	NA	NA	NA
4n rescue ES	30	2	0	NA	NA	NA

NA, not applicable.
[a]In some experiments, fetuses were delivered by cesarean section at 19.5 dpc.
[b]Number of live pups on the next day after birth.

istics of germline cells. Possibly, the interaction with Sertoli cells normally directs germ cells to spermatogenesis and inhibits multilineage differentiation in the testis. However, when germline cells are continuously stimulated to expand in the absence of Sertoli cells, as in our culture conditions, germ cells may be released from this inhibition and some of the cells converted to pluripotent cells. Teratogenesis from germline cells is susceptible to environmental influences; for example, teratoma formation can be significantly enhanced (~10-fold) in vivo by ectopic transplantation of the fetal genital ridge (Stevens, 1984). As PGCs can become pluripotential only after in vitro culture and cytokine supplementation was also necessary for EG cell conversion (Matsui et al., 1992; Resnick et al., 1992), growth stimulation and release from somatic cells may modify the differentiation program of germline cells.

Several lines of evidence in our study provide support for the multipotential nature of spermatogonial stem cells. First, we did not find PGC-like germ cells in the neonatal testis, and we failed to induce mGS cells from neonatal testis in EG cell culture conditions (mSCF + LIF + bFGF). Therefore, the mGS cells arose through a different mechanism from that of EG cells, and the results suggest that PGC-like cells in neonatal testis, if any, are not responsible for the generation of mGS cells. Second, results of p53 knockout mouse experiments showed that mGS cells develop from GS cells. The use of the p53 knockout mouse was based on previous studies that showed an increased frequency of teratoma in this strain; it is estimated that loss of the *p53* gene results in a 100-fold increase in the susceptibility to testicular teratoma (Lam and Nadeau, 2003). Nevertheless, GS cells from this strain were phenotypically similar to wild-type spermatogonia and could produce normal-appearing spermatogenesis when transferred into seminiferous tubules. In this sense, they are indistinguishable from wild-type GS cells and fulfill the criteria for spermatogonial stem cells. Using this model, we found that the partial androgenetic imprint in mGS cells occurred with loss of the androgenetic imprint in GS cells. Perhaps the same is true of wild-type mGS cells; the partial androgenetic imprint patterns may not indicate the origin of mGS cells directly but rather reflect epigenetic instability in vitro, as reported for ES/EG cells (Labosky et al., 1994; Dean et al., 1998; Humpherys et al., 2001). Although these results are based on a mutant mouse model, they strongly suggest that GS cells are multipotential or can acquire multipotentiality by loss of a single gene. Spontaneous teratomas in mice occur almost exclusively in the 129/Sv background and are considered to develop from PGCs (Stevens, 1984). However, our results strongly suggest that spermatogonial stem cells are multipotential.

Interestingly, the acquisition of multipotentiality in mGS cells was concurrent with the loss of spermatogonial stem cell potential. Despite their testicular origin, mGS cells formed teratomas in the seminiferous tubules, indicating that this environment was no longer sufficient for spermatogenesis after the cells became pluripotent. This contrasts with GS cells, which produce spermatogenesis on transfer to the seminiferous tubules (Kanatsu-Shinohara et al., 2003a). Therefore, mGS cells are more closely related to ES/EG cells in terms of cell function. The reason for the loss of spermatogonial stem cell potential is unknown; however, we speculate that it may be related to the loss of responsiveness to GDNF during the course of the establishment of mGS cells, as GDNF is essential for the self-renewing division of spermatogonial stem cells (Meng et al., 2000). Another question that remains to be answered is why GS cells converted to mGS cells only at early passages. In our experiments, mGS cells appeared within 7 weeks of culture initiation but not at later stages. Once established, however, GS cells were stably committed to the germline, because we did not observe any mGS cell conversion when they were expanded in large-scale culture or transplanted in vivo. The loss of multipotentiality might be ascribed to the nonoptimal culture condition; it is widely known that ES cells differentiate easily and lose germline potential in the absence of LIF (Smith, 2001). Likewise, germline cells may tend to lose somatic cell potential in nonoptimal culture conditions. In this sense, it is interesting that, in contrast to mGS cells from wild-type mice, mGS cells developed in the long-term in p53 knockout mice. Although the mechanism for the maintenance or loss of multipotentiality of germline cells is currently unclear, the results suggest that this gene is involved in these processes, and GS cells from p53 knockout mice may be useful for analyzing how germline cells retain multipotentiality.

The most striking result from our experiments is the contribution of mGS cells to normal embryo development. Donor cell makers were present in various parts of the body, including the germline cells. These results demonstrate that mGS cells not only produce tumors but also can contribute to normal embryonic development. However, the function of the cells may not be completely

normal, because we could not recover live offspring in tetraploid complementation experiments, which indicates that mGS cells alone cannot produce a normal whole embryo. The failure is most likely related to the imprint status of mGS cells, since altered imprinted gene methylation causes fetal abnormalities with ES cells (Dean et al., 1998; Surani, 2001). Nevertheless, the imprint status of mGS cells did not influence the germline competence, and normal offspring were obtained from the chimeric animal. This agrees with the previous reports that both ES and EG cells can produce germline chimera (Robertson and Bradley, 1986; Labosky et al., 1994; Stewart et al., 1994), even with androgenetic imprint patterns (Narasimha et al., 1997).

The derivation of multipotent stem cells from the neonatal testis may have practical value for medicine and biotechnology. These cells are different from other reported multipotent cells in terms of morphology, marker expression, and capacity for differentiation (Verfaillie, 2002; Wagers and Weissman, 2004). While it is important to study the biology of individual cell types and assess their potential for clinical application, a major advantage of mGS cells is that techniques currently used to derive specific lineages of cells from ES cells are applicable directly. Clearly, the derivation of mGS cells has fewer ethical concerns than does the derivation of ES cells, because mGS cells can be obtained without sacrificing the conceptus or embryos. Furthermore, the availability of histocompatible, multipotent tissue for autotransplantation would circumvent immunological problems associated with ES cell-based technology. Although we failed to obtain mGS cells from mature wild-type animals, this was likely due to the low success rate of GS cell establishment. The results of the p53 knockout mouse experiment suggest that mGS cells can arise from mature testis. Development of more efficient systems to derive GS cells from mature testis is necessary at this stage of research, and suppression of p53 expression in GS cells, such as by RNA interference, may be useful for enhancing the frequency of derivation. Future studies should also be directed toward examining the effect of imprinting on the range and efficiency of differentiation. Such studies will provide important information for potential clinical applications.

Experimental Procedures

Cell Culture

Testis cells were collected from newborn (0–2 days old) ddY or DBA/2 mice (Japan SLC, Shizuoka, Japan). For some experiments, testis cells were collected from a newborn Green mouse (Kanatsu-Shinohara et al., 2003a) or p53 knockout mouse in ICR background (Tsukada et al., 1993). Testis cell culture was performed according to the previously published protocol (Kanatsu-Shinohara et al., 2003a), with slight modifications. In brief, testis cells were allocated to a gelatin-coated tissue culture plate (2×10^6 cells/3.8 cm^2). The next day, floating cells were recovered and passed to secondary culture plates. After 7 days in culture, the cells were passed to a fresh culture plate at a 1:2 dilution. When the cells were confluent (~7 days after the second passage), they were passed again (1:1 dilution). At the third or fourth passage, the cells were maintained on mitomycin C-inactivated MEF. ES-like cells were cultured in Dulbecco's modified Eagle's medium supplemented with 15% FCS, 5×10^{-5} M 2-mercaptoethanol, and 10^3 units/ml ESGRO (Invitrogen, Carlsbad, CA). To induce EG cells from neonatal testis, the same medium was also supplemented with 20 ng/ml human bFGF (Invitrogen), and cells were cultured on SI⁴-m220 (gift from Dr. T. Nakano, Osaka University).

For adult testis culture, 2×10^7 cells from 3- to 8-week-old wild-type and p53 knockout mice were used to recover spermatogonial stem cells with anti-CD9 antibody as described elsewhere (Kanatsu-Shinohara et al., 2004), and selected cells were plated on gelatin-coated plate (3×10^5 cells/9.5 cm^2). GS cell colonies were picked by micromanipulation and transferred to MEF for expansion.

Standard ES cell medium was used to culture D3 ES cells that ubiquitously express the EGFP gene under the CAG promoter (provided by Dr. M. Okabe, Osaka University; Niwa et al., 1991).

Antibodies and Staining

The following primary antibodies were used: rat anti-EpCAM (G8.8), mouse anti-SSEA-1 (MC-480), mouse anti-sarcomeric protein (MF20; Developmental Studies Hybridoma Bank, University of Iowa), rat anti-mouse Forssman antigen (M1/87), rat anti-human α6-integrin (GoH3), biotinylated hamster anti-rat β1-integrin (Ha2/5), biotinylated rat anti-mouse CD9 (KMC8), allophycocyanin (APC)-conjugated rat anti-mouse c-kit (2B8), rat anti-mouse CD31 (MEC 13.3), phycoerythrin (PE)-conjugated rat anti-mouse Ter119 (TER-119), biotinylated rat anti-mouse Mac1 (M1/70), biotinylated rat anti-mouse Gr1 (RB6-8C5), rat anti-mouse VE-cadherin (11D4.1), APC-conjugated rat anti-mouse CD45 (30-F11; BD Biosciences), rat anti-TDA (EE2; provided by Dr. Y. Nishimune, Osaka University), APC-conjugated rat anti-mouse Flk-1 (Avas 12α1; provided by Dr. S. Nishikawa, RIKEN), goat anti-mouse cardiac troponin-I (cTn-I) (Santa Cruz Biotechnology, Santa Cruz, CA), mouse anti-human myosin light chain 2v (MLC2v) (Alexis Biochemicals Inc, Montreal, Canada), rabbit anti-mouse atrial natriuretic peptide (ANP) (Protos Biotech Corporation, NY), mouse anti-human myelin basic protein (MBP) (Pm43), rabbit anti-glial fibrillary acidic protein (GFAP), rabbit anti-mouse tyrosine hydroxylase (TH), and mouse anti-human β-tubulin III (Tuj) (SDL.3D10) (Sigma, St. Louis, MO). APC-conjugated goat anti-rat-IgG (Cedarlane Laboratories, ON, Canada), APC-conjugated streptavidin (BD Biosciences), Alexa Fluor 488-conjugated goat anti-mouse IgG, Alexa Fluor 647-conjugated goat anti-rat IgM, Alexa Fluor 633-conjugated goat anti-mouse IgM (Molecular Probes, Eugene, OR), Cy3-conjugated donkey anti-mouse IgG, Cy3-conjugated donkey anti-rabbit IgG, ALP or peroxidase-conjugated donkey anti-mouse IgG, ALP-conjugated donkey anti-rabbit IgG (Jackson Immunoresearch, West Grove, PA), ALP-conjugated rabbit anti-goat IgG (Vector Laboratories, Burlingame, CA), or ALP-conjugated goat anti-rat IgG (Chemicon) were used as secondary antibodies. The cell staining and analysis was carried out with a FACSCalibur system (BD Biosciences) (Kanatsu-Shinohara et al., 2003a). ALP or DAB staining was carried out using a VECTOR alkaline phosphatase substrate kit or DAB substrate kit (Vector Laboratories), respectively, according to manufacturer's protocol.

Differentiation into Specific Lineages In Vitro

For differentiation into mesodermal lineages, ES-like cells were cultured on OP9 feeder layers, and cell differentiation was induced as described (Nishikawa et al., 1998; Schroeder et al., 2003, Hirashima et al., 1999). Vascular cells were identified by the uptake of DiI-acetylated low-density lipoprotein (Molecular Probes). Methylcellulose culture was performed as described previously (Nishikawa et al., 1998). All cytokines were provided by Kirin Brewery (Tokyo, Japan). Neural cell differentiation was induced as previously described (Ying et al., 2003).

Analysis of Marker Gene Expression

RT-PCR for Nanog, Rex-1, ERas, Esg-1, Cripto, and ZFP57 were carried out using specific primers, as described (Mitsui et al., 2003; Goolsby et al., 2003; Takahashi et al., 2003; Tanaka et al., 2002; Kimura et al., 2001; Ahn et al., 2004). PCR amplifications for Oct-4, UTF1, and HPRT were carried out by using specific primers (5′-AGCTGCTGAAGCAGAAGAGG-3′ and 5′-GGTTCTCATTGTTGTCG GCT-3′ for Oct-4, 5′-GATGTCCCGGTGACTACGTCT-3′ and 5′-TCG GGGAGGATTCGAAGGTAT-3′ for UTF1, and 5′-GCTGGTGAAAAG GACCTCT -3′ and 5′- CACAGGACTAGAACACCTGC-3′ for HPRT).

Analysis of Imprinted Genes

Bisulfite genomic sequencing of DMRs of imprinted genes was carried out as described (Lee et al., 2002). PCR amplifications of each DMR region from bisulfite-treated genomic DNAs was carried out by using specific primers (5′-GGAATATTTGTGTTTTTGGAGGG-3′ and 5′-AATTTGGGTTGGAGATGAAAATATTG-3′ for *H19*, 5′-GGTTTGGTATATATGGATGTATTGTAATATAGG-3′ and 5′-ATAAAACACCAAATCTATACCAAAATATACC-3′ for *Meg3 IG*, 5′-GTGTAGAATATGGGGTTGTTTTATATTG-3′ and 5′-ATAATACAACAACAACAACAATAACAATC-3′ for *Rasgrf1*, 5′-TTAGTGGGGTATTTTTATTTGTATGG-3′ and 5′-AAATATCCTAAAAATACAAACTACACAA-3′ for *Igf2r*, 5′-GTAAAGTGATTGGTTTTGTATTTTTAAGTG-3′ and 5′-TTAATTACTCTCCTACAACTTTCCAAATT-3′ for *Peg10*, and 5′- GGTTTTTTAGAG GATGGTTGAGTG-3′ and 5′- TCCAACCCTACTAACCCATCACC-3′ for *Oct-4*). The DNA sequences were determined in both directions. For COBRA, PCR products were digested with restriction enzymes with a recognition sequence containing CpG in the original unconverted DNA (Xiong and Laird, 1997). Intensity of digested DNA bands was quantified with ImageGauge software (Fuji Photo Film, Tokyo, Japan).

Transplantation

For subcutaneous injections, approximately 2×10^6 cells were injected into KSN nude mice (Japan SLC). For microinjections into the seminiferous tubules, approximately 3×10^5 cells were injected into the seminiferous tubules of an immune-suppressed W mouse (Japan SLC) recipient through the efferent duct (Kanatsu-Shinohara et al., 2003b).

Chimera Formation and Microinsemination

Cells were injected into the blastocoel of 3.5 dpc blastocysts of C57BL/6 mice using a Piezo-driven micromanipulator (Kimura and Yanagimachi, 1995). The blastocysts were returned to the oviducts or uteri of 2.5 dpc pseudopregnant ICR foster mothers on the day of microinjection. Tetraploid embryo aggregation chimeras were produced using the method developed by Nagy et al. (1993), except that two-cell blastomeres were electrofused by applying an electric pulse (2500 V/cm, 10 μsec) in 300 mM mannitol solution. Microinsemination was carried out as described using BDF1 oocytes (Kimura and Yanagimachi, 1995). The embryos were transferred on the next day after culture.

Histology

Tissues were fixed in 10% formalin and processed for paraffin sectioning. Chimeric embryos were fixed in 4% paraformaldehyde and frozen in Tissue-Tek OCT compound (Sakura Finetechnical, Tokyo, Japan) for cryosectioning. Slides were analyzed with an Olympus confocal laser scanning microscope.

Acknowledgments

We declare that none of the authors have a financial interest related to this work. We thank Drs. Y. Kaziro and Y. Matsui for discussion and encouragement, and Ms. A. Wada for technical assistance. Financial support for this research was provided by the Inamori Foundation; the Ministry of Health and Welfare; and the Ministry of Education, Culture, Sport, Science, and Technology of Japan.

Received: April 30, 2004
Revised: October 7, 2004
Accepted: November 2, 2004
Published: December 28, 2004

References

Ahn, J.-I., Lee, K.-H., Shin, D.-M., Shim, J.-W., Lee, J.-S., Chang, S.Y., Lee, Y.-S., Brownstein, M.J., Lee, S.-H., and Lee, Y.-S. (2004). Comprehensive transcriptome analysis of differentiation of embryonic stem cells into midbrain and hindbrain neurons. Dev. Biol. *265*, 491–501.

Anderson, R., Schaible, K., Heasman, J., and Wylie, C.C. (1999). Expression of the homophilic adhesion molecule, Ep-CAM, in the mammalian germ line. J. Reprod. Fertil. *116*, 379–384.

Brinster, R.L., and Avarbock, M.R. (1994). Germline transmission of donor haplotype following spermatogonial transplantation. Proc. Natl. Acad. Sci. USA *91*, 11303–11307.

Brinster, R.L., and Zimmermann, J.W. (1994). Spermatogenesis following male germ-cell transplantation. Proc. Natl. Acad. Sci. USA *91*, 11298–11302.

Chambers, I., Colby, D., Robertson, M., Nichols, J., Lee, S., Tweedie, S., and Smith, A. (2003). Functional expression cloning of Nanog, a pluripotency sustaining factor in embryonic stem cells. Cell *113*, 643–655.

Davis, T.L., Trasler, J.M., Moss, S.B., Yang, G.J., and Bartolomei, M.S. (1999). Acquisition of the H19 methylation imprint occurs differentially on the parental alleles during spermatogenesis. Genomics *58*, 18–28.

Davis, T.L., Yang, G.J., McCarrey, J.R., and Bartolomei, M.S. (2000). The H19 methylation imprint is erased and re-established differentially on the parental alleles during male germ cell development. Hum. Mol. Genet. *9*, 2885–2894.

Dean, W., Bowden, L., Aitchison, A., Klose, J., Moore, T., Menesses, J.J., Reik, W., and Feil, R. (1998). Altered imprinted gene methylation and expression in completely ES cell-derived mouse fetuses: association with aberrant phenotypes. Development *125*, 2273–2282.

de Rooij, D.G., and Russell, L.D. (2000). All you wanted to know about spermatogonia but were afraid to ask. J. Androl. *21*, 776–798.

Evans, M.J., and Kaufman, M.H. (1981). Establishment in culture of pluripotential cells from mouse embryos. Nature *292*, 154–156.

Goolsby, J., Marty, M.C., Heletz, D., Chiappelli, J., Tashko, G., Yarnell, D., Fishman, P.S., Dhib-Jalbut, S., Bever, C.T., Jr., and Trisler, D. (2003). Hematopoietic progenitors express neural genes. Proc. Natl. Acad. Sci. USA *100*, 14926–14931.

Hattori, N., Nishino, K., Ko, Y.-G., Hattori, N., Ohgane, J., Tanaka, S., and Shiota, K. (2004). Epigenetic control of mouse Oct-4 gene expression in embryonic stem cells and trophoblast stem cells. J. Biol. Chem. *279*, 17063–17069.

Hirashima, M., Kataoka, H., Nishikawa, S., Matsuyoshi, N., and Nishikawa, S.-I. (1999). Maturation of embryonic stem cells into endothelial cells in an in vitro model of vasculogenesis. Blood *93*, 1253–1263.

Humpherys, D., Eggan, K., Akutsu, H., Hochedlinger, K., Rideout, W.M., III, Biniszkiewicz, D., Yanagimachi, R., and Jaenisch, R. (2001). Epigenetic instability in ES cells and cloned mice. Science *293*, 95–97.

Kafri, T., Ariel, M., Brandeis, M., Shemer, R., Urven, L., McCarrey, J.R., Ceder, H., and Razin, A. (1992). Developmental pattern of gene-specific DNA methylation in the mouse embryo and germ line. Genes Dev. *6*, 705–714.

Kanatsu, M., and Nishikawa, S.-I. (1996). In vitro analysis of epiblast tissue potency for hematpoietic cell differentiation. Development *122*, 823–830.

Kanatsu-Shinohara, M., Ogonuki, N., Inoue, K., Miki, H., Ogura, A., Toyokuni, S., and Shinohara, T. (2003a). Long-term proliferation in culture and germline transmission of mouse male germline stem cells. Biol. Reprod. *69*, 612–616.

Kanatsu-Shinohara, M., Ogonuki, N., Inoue, K., Ogura, A., Toyokuni, S., Honjo, T., and Shinohara, T. (2003b). Allogeneic offspring produced by male germ line stem cell transplantation into infertile mouse testis. Biol. Reprod. *68*, 167–173.

Kanatsu-Shinohara, M., Toyokuni, S., and Shinohara, T. (2004). CD9 is a surface marker on mouse and rat male germline stem cells. Biol. Reprod. *70*, 70–75.

Kimura, Y., and Yanagimachi, R. (1995). Mouse oocytes injected with testicular spermatozoa or round spermatids can develop into normal offspring. Development *121*, 2397–2405.

Kimura, C., Shen, M.M., Takeda, N., Aizawa, S., and Matsuo, I. (2001). Complementary functions of Otx2 and Cripto in initial patterning of mouse epiblast. Dev. Biol. *235*, 12–32.

Koshimizu, U., Nishioka, H., Watanabe, D., Dohmae, K., and Nishimune, Y. (1995). Characterization of a novel spermatogenic cell antigen specific for early stages of germ cells in mouse testis. Mol. Reprod. Dev. *40*, 221–227.

Labosky, P.A., Barlow, D.P., and Hogan, B.L.M. (1994). Mouse embryonic germ (EG) cell lines: transmission through the germline and differences in the methylation imprint of insulin-like growth factor 2 receptor (Igf2r) gene compared with embryonic stem (ES) cell lines. Development *120*, 3197–3204.

Lam, M.-Y.J., and Nadeau, J.H. (2003). Genetic control of susceptibility to spontaneous testicular germ cell tumors in mice. APMIS *111*, 184–191.

Lee, J., Inoue, K., Ono, R., Ogonuki, N., Kohda, T., Kaneko-Ishino, T., Ogura, A., and Ishino, F. (2002). Erasing genomic imprinting memory in mouse clone embryos produced from day 11.5 primordial germ cells. Development *129*, 1807–1817.

Liu, X., Wu, H., Loring, J., Hormuzdi, S., Disteche, C.M., Bornstein, P., and Jaenisch, R. (1997). Trisomy eight in ES cells is a common potential problem in gene targeting and interferes with germ line transmission. Dev. Dyn. *209*, 85–91.

Longo, L., Bygrave, A., Grosveld, F.G., and Pandolfi, P.P. (1997). The chromosome make-up of mouse embryonic stem cells is predictive of somatic and germ cell chimaerism. Transgenic Res. *6*, 321–328.

Martin, G.R. (1981). Isolation of a pluripotent cell line from early mouse embryos cultured in medium conditioned by teratocarcinoma stem cells. Proc. Natl. Acad. Sci. USA *78*, 7634–7638.

Matsui, Y., Zsebo, K., and Hogan, B.L.M. (1992). Derivation of pluripotential embryonic stem cells from murine primordial germ cells in culture. Cell *70*, 841–847.

Meistrich, M.L., and van Beek, M.E.A.B. (1993). Spermatogonial stem cells. In Cell and Molecular Biology of the Testis, C. Desjardins, and L.L. Ewing, eds. (New York: Oxford University Press), pp. 266–295.

Meng, X., Lindahl, M., Hyvönen, M.E., Parvinen, M., de Rooij, D.G., Hess, M.W., Raatikainen-Ahokas, A., Sainio, K., Rauvala, H., Lakso, M., et al. (2000). Regulation of cell fate decision of undifferentiated spermatogonia by GDNF. Science *287*, 1489–1493.

Mitsui, K., Tokuzawa, Y., Itoh, H., Segawa, K., Murakami, M., Takahashi, K., Maruyama, M., Maeda, M., and Yamanaka, S. (2003). The homeoprotein Nanog is required for maintenance of pluripotency in mouse epiblast and ES cells. Cell *113*, 631–642.

Nagy, A., Rossant, J., Nagy, R., Abramow-Newerly, A., and Roder, J.C. (1993). Derivation of completely cell culture-derived mice from early-passage embryonic stem cells. Proc. Natl. Acad. Sci. USA *90*, 8424–8428.

Nakano, T., Kodama, H., and Honjo, T. (1994). Generation of lymphohematopoietic cells from embryonic stem cells in culture. Science *265*, 1098–1101.

Narasimha, M., Barton, S.C., and Surani, M.A. (1997). The role of the paternal genome in the development of the mouse germ line. Curr. Biol. *7*, 881–884.

Nishikawa, S.-I., Nishikawa, S., Hirashima, M., Matsuyoshi, N., and Kodama, H. (1998). Progressive lineage analysis by cell sorting and culture identifies FLK1$^+$VE-cadherin$^+$ cells at a diverging point of endothelial and hemopoietic lineages. Development *125*, 1747–1757.

Niwa, H., Yamamura, K., and Miyazaki, J. (1991). Efficient selection for high-expression transfectants with a novel eukaryotic vector. Gene *108*, 193–200.

Okuda, A., Fukushima, A., Nishimoto, M., Orimo, A., Yamagishi, T., Nabeshima, Y., Kuro-o, M., Nabeshima, Y., Boon, K., Keaveney, M., et al. (1998). UTF1, a novel transcriptional coactivator expressed in pluripotent embryonic stem cells and extra-embryonic cells. EMBO J. *17*, 2019–2032.

Pesce, M., and Schöler, H.R. (2001). Oct-4: gatekeeper in the beginning of mammalian development. Stem Cells *19*, 271–278.

Resnick, J.L., Bixler, L.S., Cheng, L., and Donovan, P.J. (1992). Long-term proliferation of mouse primordial germ cells in culture. Nature *359*, 550–551.

Robertson, E.J., and Bradley, A. (1986). Production of permanent cell lines from early embryos and their use in studying developmental problems. In Experimental Approaches to Mammalian Embryonic Development, J. Rossant, and R.A. Pedersen, eds. (Cambridge: Cambridge University Press), pp. 475–508.

Schrans-Stassen, B.H.G.J., van de Kant, H.J.G., de Rooij, D.G., and van Pelt, A.M.H. (1999). Differential expression of c-kit in mouse undifferentiated and differentiating type A spermatogonia. Endocrinology *140*, 5894–5900.

Schroeder, T., Fraser, S.T., Ogawa, M., Nishikawa, S., Oka, C., Bornkamm, G.W., Nishikawa, S.-I., Honjo, T., and Just, U. (2003). Recombination signal sequence-binding protein Jκ alters mesodermal cell fate decisions by suppressing cardiomyogenesis. Proc. Natl. Acad. Sci. USA *100*, 4018–4023.

Smith, A.G. (2001). Embryo-derived stem cells: of mice and men. Annu. Rev. Cell Dev. Biol. *17*, 435–462.

Solter, D., and Knowles, B.B. (1978). Monoclonal antibody defining a stage-specific mouse embryonic antigen (SSEA-1). Proc. Natl. Acad. Sci. USA *75*, 5565–5569.

Stevens, L.C. (1984). Spontaneous and experimentally induced testicular teratomas in mice. Cell Differ. *15*, 69–74.

Stevens, L.C., and Mackensen, J.A. (1961). Genetic and environmental influences on teratocarcinoma in mice. J. Natl. Cancer Inst. *27*, 443–453.

Stewart, C.L., Gadi, I., and Bhatt, H. (1994). Stem cells from primordial germ cells can reenter the germline. Dev. Biol. *161*, 626–628.

Surani, M.A. (2001). Reprogramming of genome function through epigenetic inheritance. Nature *414*, 122–128.

Takahashi, K., Mitsui, K., and Yamanaka, S. (2003). Role of ERas in promoting tumor-like properties in mouse embryonic stem cells. Nature *423*, 541–545.

Tanaka, T.S., Kunath, T., Kimber, W.L., Jaradat, S.A., Stagg, C.A., Usuda, M., Yokota, T., Niwa, H., Rossant, J., and Ko, M.S.H. (2002). Gene expression profiling of embryo-derived stem cells reveals candidate genes associated with pluripotency and lineage specificity. Genome Res. *12*, 1921–1928.

Tsukada, T., Tomooka, Y., Takai, S., Ueda, Y., Nishikawa, S.-I., Yagi, T., Tokunaga, T., Takeda, N., Suda, Y., Abe, S., et al. (1993). Enhanced proliferative potential in culture of cells from p53-deficient mice. Oncogene *8*, 3313–3322.

Verfaillie, C.M. (2002). Adult stem cells: assessing the case for pluripotency. Trends Cell Biol. *12*, 502–508.

Wagers, A.J., and Weissman, I.L. (2004). Plasticity of adult stem cells. Cell *116*, 639–648.

Xiong, Z., and Laird, P.W. (1997). COBRA: a sensitive and quantitative DNA methylation assay. Nucleic Acids Res. *25*, 2532–2534.

Ying, Q.L., Stavridis, M., Griffiths, D., Li, M., and Smith, A. (2003). Conversion of embryonic stem cells into neuroectodermal precursors in adherent monoculture. Nat. Biotechol. *21*, 183–186.

DTD 5

Available online at www.sciencedirect.com
SCIENCE DIRECT®

Theriogenology

ELSEVIER

Theriogenology xxx (2004) xxx–xxx

www.elsevier.com/locate/theriogenology

Birth of mice after in vitro fertilization using C57BL/6 sperm transported within epididymides at refrigerated temperatures

K. Mochida[a], M. Ohkawa[a], K. Inoue[a], D.M. Valdez Jr[b], M. Kasai[b], A. Ogura[a,*]

[a]*RIKEN Bioresource Center, Koyadai, 3-1-1 Koyadai, Tsukuba, Ibaraki 305-0074, Japan*
[b]*College of Agriculture, Kochi University, Nankoku, Kochi 783-8502, Japan*

Received 17 July 2004

Abstract

The transportation of cryopreserved spermatozoa is an economical, efficient, and safe method for the distribution of mouse strains from one facility to another. However, spermatozoa from some strains, including C57BL/6 (B6), are very sensitive to freezing and thawing and frequently fail to fertilize eggs by conventional in vitro fertilization methods at the recipient mouse facility. Since many genetically engineered mice have the B6 genetic background, this sensitivity poses a major obstacle to studies of mouse genetics. We investigated the feasibility of transporting spermatozoa within epididymides under non-freezing conditions. First, we examined the interval that B6 and B6D2F1 (BDF1) spermatozoa retained their ability to fertilize when stored within epididymides at low temperatures (5 °C or 7 °C). Fertilization rates were >50%, irrespective of the spermatozoa used, when epididymides were stored for 3 d at 7 °C. B6 spermatozoa, but not BDF1 sperm, had better retention of fertilizing ability at 7 °C versus 5 °C. We then transported freshly collected B6 and BDF1 epididymides from a sender colony to a recipient colony using a common package delivery service, during which the temperature was maintained at 5 °C or 7 °C for 2 d. Sufficiently high fertilization rates (68.0–77.5%) were obtained for all experimental groups, except for B6 spermatozoa transported at 5 °C. These spermatozoa were successfully cryopreserved at the recipient facility and, yielded post-thaw fertilization rates of 27.6–66.4%. When embryos derived from the B6 spermatozoa that

* Corresponding author. Tel.: +81 29 836 9165; fax: +81 29 836 9172.
E-mail address: ogura@rtc.riken.go.jp (A. Ogura).

0093-691X/$ – see front matter © 2004 Published by Elsevier Inc.
doi:10.1016/j.theriogenology.2004.11.013

THE 9468 1–9

were transported at 7 °C were transferred into recipient females, 52.7% (38/72) developed to term. In conclusion, transportation of epididymides at refrigerated temperatures is a practical method for the exchange of mouse genetic resources between facilities, especially when these facilities do not specialize in sperm cryopreservation. For the B6 mouse strain, the transportation of epididymides at 7 °C rather than 5 °C, is recommended.

Keywords: Cryopreservation; Epididymis; IVF; Mouse; Spermatozoa

1. Introduction

The mouse is the animal species that is most commonly used in biomedical research, owing to the availability of large amounts of information on its genetics and biology. Technical advances in mouse genetic engineering have substantially increased the research value of the mouse and greatly increased the number of available genetically modified mouse strains, including transgenic and gene-targeted mice as the need to share these valuable genetic resources grows, strains are transferred from one facility to another with increasing frequency. However, the transportation of live mice is very costly, and there is an increased risk of spreading diseases in recipient colonies. The transportation of cryopreserved embryos and spermatozoa is the current preferred method for the exchange of mouse strains because it avoids the problems associated with handling live animals [1]. The recent development of rapid and easy-freezing methods has significantly improved embryo/sperm cryopreservation techniques [2–5]. Although this should have enabled widespread transportation of cryopreserved embryos and sperm between mouse facilities, conventional live mouse transportation is still commonly employed. This is mainly due to the technical requirements for transporting frozen materials; both the sending and receiving facilities should specialize in freeze-thaw methods, and the embryos/spermatozoa should be kept in liquid nitrogen during transportation. Furthermore, for some of the most commonly used inbred strains, including C57BL/6 (B6), fertilization rates using frozen-thawed spermatozoa are generally at the low end of desirability in terms of establishing mouse colonies [1,4,6], although this problem can be overcome by special micromanipulative techniques (intracytoplasmic sperm injection [7] and partial zona dissection [8]). This is a major obstacle for the widespread exchange of cryopreserved spermatozoa because many useful genetically modified mice have the B6 genetic background. Recently, the potential for storage of gametes and gonadal tissues under non-freezing conditions has been recognized in several species [9–15]. The method does not require specialized freezing devices or technical skills. Even mouse spermatozoa that have been retrieved postmortem and stored at low temperature for a few days can subsequently be used to fertilize oocytes, and the resultant embryos develop normally [9,15]. We wanted to assess the feasibility of transporting spermatozoa under non-freezing conditions as an alternative to shipping cryopreserved spermatozoa. For this purpose, we transported fresh epididymides of B6 males by commercial courier under refrigeration, and examined the fertilizing ability of the spermatozoa at the recipient laboratory.

2. Materials and methods

2.1. Preparation of epididymides

We used fully mature C57BL/6Cr Slc (B6) and B6D2F1 (BDF1) males (SLC Co. Ltd., Shizuoka, Japan) aged 3–12 months. The mice were sacrificed by cervical dislocation, and the cauda epididymides were removed, together with a part of the corpus epididymis and vas deferens. Each epididymis was stored in a 1.8-mL cryotube (no. 363401; Nunc, Roskilde, Denmark) that contained ~0.5 mL mineral oil (M-8410; Sigma Chemical Co., St. Louis, MO, USA) or silicone oil (no. 146153; Sigma Chemical Co.) at two different temperatures, 5 °C or 7 °C. In vitro fertilization (IVF) was attempted 1–4 d later. The experiments were performed with two or three replicates.

2.2. Transportation of epididymides

For the transportation experiments, fresh cauda epididymides were placed into a 1.8-mL cryotube that contained ~0.5 mL mineral oil. The cryotubes were packed in plastic bags with a small temperature data logger (Thermochron; OnSolution Pty Ltd., Sydney, Australia), and then placed in a thermos that contained water at 5 °C or 7 °C. The samples were transported under refrigeration from Kochi to Tsukuba (a distance of about 900 km) using a commercial courier service. The epididymides were delivered to the recipient facility and were stored overnight at the transportation temperature, in order to conduct IVF experiments according to our standard experimental schedule. The total duration of epididymal storage was ~48 h, including transportation. The experiments were performed in triplicate.

2.3. In vitro fertilization

Cauda epididymides that had been refrigerated for 1–4 d or transported (with a total refrigerated storage time of 48 h) were used for IVF. Spermatozoa from each epididymis were suspended in 450 μL human tubal fluid (HTF) medium that contained 0.5% bovine serum albumin, covered with silicone oil (Sigma Chemical Co.), and pre-incubated at 37 °C under 5% CO_2 in air for 1–2 h. Superovulation was induced in females of the same strain as the male, by treatment with 7.5 IU pregnant mare's serum gonadotropin (PMSG; Peamex, Sankyo Co., Tokyo, Japan), followed 48–54 h later by 7.5 IU human chorionic gonadotropin (hCG, Puberogen; Sankyo Co., Tokyo, Japan). Cumulus-oocyte complexes were collected from the oviducts and placed into 80-μL drops of HTF under silicone oil.

Insemination was carried out by adding a small drop of sperm suspension to these HTF drops (final sperm concentration of ~5×10^5 cells/mL). Four to six hours after insemination, the eggs were removed from the fertilization drops, washed in PB1 medium, and cultured overnight in 10–20-μL drops of glucose-containing CZB medium [16]. The next morning, the number of two-cell embryos was scored, and the embryos were either cultured through to the blastocyst stage or surgically transferred into the oviducts of pseudopregnant ICR mice (CLEA Japan Inc., Tokyo, Japan) for the evaluation of in vivo development. Recipients were allowed to deliver their young. After weaning, the mothers were sacrificed and implantation sites examined.